AD NUMBER
AD360625
CLASSIFICATION CHANGES
TO: unclassified
FROM: secret
LIMITATION CHANGES
TO: Approved for public release, distribution unlimited
FROM: Distribution authorized to DoD only; Test and Evaluation; 23 JUN 1961. Other requests shall be referred to Defense Atomic Support Agency, Washington, DC. Formerly Restricted Data.
AUTHORITY
dna ltr dtd 3 oct 1995; dna ltr dtd 3 oct 1995

SECRET

WT-1611

This document consists of 74 pages.

No. 165 of 175 copies, Series A

Operation

HARDTACK

April - October 1958

OPERATION HARDTACK—PROJECT 1.6

WATER-WAVE MEASUREMENTS (U)

Issuance Date: June 23, 1961

HEADQUARTERS FIELD COMMAND
DEFENSE ATOMIC SUPPORT AGENCY
SANDIA BASE, ALBUQUERQUE, NEW MEXICO

FORMERLY RESTRICTED DATA

Handle as Restricted Data in foreign dissemination. Section 144b, Atomic Energy Act of 1954.

This material contains information affecting the national defense of the United States within the meaning of the espionage laws Title 18, U. S. C., Secs. 793 and 794, the transmission or revelation of which in any manner to an unauthorized person is prohibited by law.

SECRET

Inquiries relative to this report may be made to

Chief, Defense Atomic Support Agency
Washington 25, D. C.

When no longer required, this document may be destroyed in accordance with applicable security regulations.

DO NOT RETURN THIS DOCUMENT

USAEC Office of Technical Information Extension
Oak Ridge, Tennessee

WT-1611

OPERATION HARDTACK—PROJECT 1.6

WATER-WAVE MEASUREMENTS (U)

Lewis W. Kidd, Project Officer
Rockne H. Johnson

Scripps Institution of Oceanography
University of California
La Jolla, California

ABSTRACT

The objectives were to study wave generation mechanisms for two underwater shots, Wahoo and Umbrella, and to examine the terminal effects of these waves by inundation studies. These studies were to be integrated with the results of previous nuclear explosions under related geometries to the end that rational prediction might be made of the water waves resulting from future nuclear explosions.

Instrumentation for these shots consisted of various types of underwater pressure-time recorders, shipboard-mounted gyro-referenced inclinometers, cameras, and inundation gages. Instrument failure was very high for Wahoo; however, Umbrella was more successfully documented.

Results of Wahoo have been deduced primarily from a photographic record of the motion of a deep-moored floating station (coracle) supplemented by pieces of information from other incomplete records. The piecing together of the data allowed a reasonably reliable extrapolation to the first node of the wave envelope for a deep water record at 4,500 feet range from surface zero.

This record was compared with the theory in Reference 1 and found to give very good agreement for source conditions of a parabolic depression with a 213-foot initial depth and a 940-foot radius. Photographs of the plume at +7 seconds corroborate this lateral dimension.

Because Wigwam was the only other nuclear shot which could be readily compared with Wahoo, the results from that shot were closely reexamined and the same reconstruction techniques applied as for Wahoo. Crater dimensions derived from application of the theory of Reference 1 indicated a deeper and narrower paraboloid than for Wahoo. Correlation of the theoretical wave envelope with that recorded was not as close as for Wahoo, but this can be ascribed to the fact that all the energy for the Wigwam waves was not released from surface zero at a specific time. The significant fact is that the higher group velocity measured for Wahoo waves was due to its greater crater radius despite the fact that the Wigwam waves contained more energy.

A very rough scaling relationship between Wigwam and Wahoo can be derived, but it is important to recognize the limitations of any formula based on such scanty data.

The transition from cube root to fourth root in scaling from small to large yields was explored and illustrated by means of Project Seal data.

Umbrella wave records were obtained from three pressure-time recorders at close range, two pressure-time recorders and an inclinometer at intermediate range, and a long-range pressure-time-recording shore station.

The data obtained was analyzed in the same manner as for lagoon shots in previous operations and was found to coincide with the extrapolated Operation Redwing data for a device of equal yield detonated at the surface. The enhancement of wavemaking efficiency due to submergence, which has been observed for all other underwater nuclear shots, was not observed for Umbrella. It may be hypothesized that the location of the device on the bottom allowed it to transmit much of its energy directly into the earth, as a surface shot transmits the preponderance of its energy into the atmosphere.

Inundation from Wahoo was much greater than anticipated. Inundation from Umbrella was negligible because of the protection afforded the islands by an extensive lagoon reef.

FOREWORD

This report presents the final results of one of the projects participating in the military-effect programs of Operation Hardtack. Overall information about this and the other military-effect projects can be obtained from ITR–1660, the "Summary Report of the Commander, Task Unit 3." This technical summary includes: (1) tables listing each detonation with its yield, type, environment, meteorological conditions, etc.; (2) maps showing shot locations; (3) discussions of results by programs; (4) summaries of objectives, procedures, results, etc., for all projects; and (5) a listing of project reports for the military-effect programs.

CONTENTS

Chapter 1

INTRODUCTION

1.1 OBJECTIVES

The objectives were to study wave generation mechanisms for two underwater shots, Wahoo and Umbrella, and to examine the terminal effects of these waves by inundation studies. These studies were to be integrated with the results of previous nuclear explosions under related geometries to the end that rational prediction might be made of the water waves resulting from future nuclear explosions.

1.2 BACKGROUND

1.2.1 General. The documentation of waves generated by nuclear explosions has been the objective of research projects for Operations Crossroads, Ivy, Castle, Wigwam, and Redwing. This work has always been complicated by many factors, including test-area geometry, instrument failure, and large gaps between data. Although a certain amount of empirical data was gathered applicable to particular shots, progress toward an understanding of the generative mechanism and the development of a universal scaling formula has been slow.

The bulk of pertinent data from previous nuclear tests has resulted from devices detonated on barges moored over varying depths of water within Bikini and Eniwetok lagoons. In addition to these surface shots, there were two in which the device was submerged: Shot Baker during Operation Crossroads and Shot Wigwam.

Work on a laboratory scale has also been conducted, both with small high-explosive charges and with geometrically defined initial disturbances. In such experimentation, it is possible to conduct many tests and to repeat performances that require verification. On the other hand, there are certain disadvantages: (1) the uncertainty of the relationship between the effects of chemical and nuclear explosions, and (2) complications of scaling over an extreme range of yields where the functions of such nonscaling quantities as atmospheric pressure, gravity, viscosity, and surface tension must be considered.

1.2.2 Project Seal. Project Seal was initiated by military interest in the application of offensive inundation during World War II. The most significant work was the conduct of a series of tests with small TNT charges in a basin of intermediate depth. The effect of varying the location of the charge with respect to the water surface was explored, and certain critical depths of submergence were discovered. The deeper of these, designated by the project report (Reference 2) as the "lower critical depth," corresponds to that defined in the theoretical work in Reference 3. The "upper critical depth" described in Reference 2 as "adjacent to the water surface" was discovered to exhibit a very sharp peak and to yield wave heights greater than the lower critical depth. This upper critical depth has never been predicted theoretically or verified by independent research.

1.2.3 Shot Baker. The first nuclear device to yield water waves of interest was detonated in Bikini lagoon in 1946 as Shot Baker of Operation Crossroads. Water depth in the vicinity of the 20-kt device was 150 to 160 feet, and the depth of submergence was 65 feet. This lagoon depth was comparatively much shallower than that for the Seal tests, and the depth of submergence chosen was not representative of either of the critical depths. The wave data recorded showed that approximately 1 percent of the yield was converted to water-wave energy. A model law was deduced, the significant feature of which was Hr = constant, where H is the wave height (feet) and r is the range (feet) from surface origin. The first crest was found to travel with the velocity of a solitary wave:

$$C = \sqrt{g(h + H_c)}$$

Where: C = celerity, ft/sec
g = acceleration due to gravity, ft/sec
h = water depth, feet
H_c = wave height, feet; subscript c denotes wave crest property

1.2.4 Operation Castle. Nuclear devices tested during Operation Castle for which significant data was recorded were of megaton range and located on barges in Bikini lagoon. The generated waves traveled to the wave recorders over paths that were refracted to a greater or lesser degree, which compromised the applicability of the results to a scaling law. The general indication was that the Hr product was again constant. Of perhaps greater significance, however, was the shape of the wave train revealed by the records. For Shots Union and Yankee, with yields of 7 and 13.5 Mt, respectively, the first and second crests had large amplitudes with a long shallow trough between. The shapes of the crests were suggestive of solitary waves. This was in contrast with the records of Shot Baker of Operation Crossroads where the first trough was, as often as not, of greater amplitude than either adjacent crest.

1.2.5 Waterways Experiment Station. Small scale tests with high explosives were conducted by the Corps of Engineers, U. S. Army, at the Waterways Experiment Station (WES) in 1952. These tests were intended to model the effects of detonating a 20-kt weapon in typical harbors. The ratio $h/W^{1/3}$ (where W = device yield, kilotons equivalent TNT) was assumed to be a constant for geometric similarity, and tests were conducted with a series of charge sizes for each of several scaled depths. The depth of charge submergence was also varied. The effect of scaling by an arbitrary exponent from a yield of 20 kt down to charges as small as 0.5 pound of TNT was to change the yield-depth relationships all out of proportion to those intended. The recorded waves bore no resemblance to those of Shot Baker but were of the form of the much shallower (compared to yield) Castle shots. No critical submergence was discovered, but then, the water was never so deep as the lower critical depth, and the region of the upper critical depth was not examined in detail.

1.2.6 Laboratory Studies. These included two-dimensional studies by J. E. Prins (Reference 3) of waves generated by a local uniform elevation or depression of the water surface. The initial disturbance was established by elevating or depressing the water surface in a box at one end of a long trough. The laboratory setup allowed close dimensional control. In varying the length and elevation of the initial disturbance as well as the water depth, a series of records was obtained that was very revealing as to the transitions which wave trains undergo as the generation and propagation parameters are varied. With the dimensions of the initial disturbance small as compared to the water depth, the wave train showed purely oscillatory characteristics and was similar to those observed by Project Seal for a 4.38-pound TNT charge in 13 feet of water. As the ratio of initial disturbance to depth is increased, the first crest takes on more and more of the solitary wave characteristics, both in form and velocity. This is likened to the wave generated by Shot Baker. With a further increase in the disturbance-to-depth ratio, nearly all of the energy of the wave train is contained in a first crest emanating as a solitary wave

followed by much smaller oscillations. In the extreme of the test series, the wave train was composed of two or more crests with solitary wave characteristics and no intervening troughs. In these cases, where the elevation parameter was four or five times the water depth, the complex solitary wave group was replaced at close range by a bore. This last case is considered to be the aspects of Shots Linton and Yankee as well as the [illegible] tests.

The phase speeds and periods of the recorded wave trains were compared to the dispersion theories for shallow water as derived in Reference 1 and for deep water. In most cases the agreement with the theory of Reference 1 was very good.

1.2.7 Operation Wigwam. A deep underwater shot was conducted in the open sea in 1955. The 30-kt device was submerged 2,000 feet in a general ocean depth of 15,000 feet. The oceanic environment proved a great enemy to instrumentation to the end that all wave data was extracted from photographs of surface vessels. Analysis of the derived records was based on the more significant waves, which were the only ones which could be observed by photographic methods, and was consequently incomplete. However, the character of the wave train was oscillatory, with the largest waves appearing in the middle of the group. Deep-water dispersion theory was shown to apply. The energy measurements indicated a wave-making efficiency somewhat higher than had been previously encountered.

1.2.8 Operation Redwing. The Redwing water waves report (Reference 4), based primarily on three surface shots, was able to contribute a significant amount of empirical data on the generation and propagation of water waves in Bikini lagoon. In this study the energy content and distribution for wave records from stations nearest to the various surface zeros were carefully examined and evaluated. It was concluded that the shape of the initial disturbance was a cylindrical crater, extending to the bottom of the lagoon, which was surrounded by a raised lip of water. This water crater lip, containing both potential and kinetic energy, generated the first crest of the radiating wave train, whereas the remainder of the train was generated by the potential of the crater cavity. It was assumed that the dissipation of energy from the first crest was negligible out to the range of the nearest recording station, and the energy in the recorded wave train was partitioned according to the above assumption. The energy of the waves following the first crest was equated to the energy of the crater; the depth was taken as the preshot depth for want of a better standard, and a crater radius was derived. It was allowed that this dimension may not accurately define the limits of the actual existing water crater although it was felt to be of the right order; its primary purpose was to obtain a linear dimension, which is a function of yield alone, with which to compare the several shots and obtain a scaling formula. Crater radius was found to vary as the fourth root of shot yield.

Further empirical steps allowed derivation of the following scaling formula:

$$H_c r^{0.95} = 3.44 (h_g^{1} W^{1/4})^{0.89} \quad (1.1)$$

Where: subscript g denotes generation.

In assigning the exponent to the range, considerable regard was given to the fact that Crossroads and Castle tests indicated a value of one although the Redwing results indicated a somewhat lower value. The wave height was referred to a depth of 60 feet of water, an arbitrary value.

It was observed in Reference 4 that the depth of generation and the depth of propagation are independent parameters affecting the wave height. A scaling function for depth of propagation was not derived, because all experimental data was propagated over the same depth, that of Bikini lagoon.

Energy calculations of Reference 4 also disclosed that the wave-making efficiency of Shot Baker was enhanced far beyond that of a surface shot of equal yield.

1.3 THEORY

1.3.1 General. Beginning with Cauchy and Poisson in the early 19th century, the problem

of describing the water waves generated by a local disturbance has been attacked by many people at many times. These theoretical approaches have varied principally in their consideration of the form of the initial disturbance, water depth, and the number of dimensions of freedom of water movement.

13.2 [illegible]. The most recent approach, and apparently the one most applicable to explosion problems, is the work of [illegible] (Reference 11) who consider three dimensions, water of uniform finite depth, and an initial disturbance (impulse or displacement) of general form. Solutions for several specific forms of the initial disturbance are also given. The case of initial displacement (elevation or depression) of the water surface seems most applicable to a surface explosion. The theory is not valid for application at ranges near the initial disturbance.

The requirement of the theory that the water depth be uniform can, to an extent, be adapted to actual problems by considering separately the functions of depth of generation and depth of propagation. The amplitude term is regarded as a function of the depth of generation, and the dispersion function involves the varying depth of propagation. Wave arrival times can then be obtained by numerical integration along the travel path. This adaptation loses its efficacy as the ratio of crater radius to depth of generation is increased. The varying depth under the local disturbance then becomes a significant factor and imposes directional characteristics to the wave pattern. If the explosion occurs at or near the edge of a shoal where the crater is [illegible], the depth of generation is continuously changing, because the original crater is being filled [illegible] by [illegible] generated wave motion. This situation effectively removes the problem from the realm of applicability of present theoretical models, and recourse must be had to a more empirical approach.

One phase of Reference 11 that has been shown to represent the recorded data even in shallow depths is the dispersion function, which relates wave period to time and range. This has been [illegible] by References [illegible] and 15. The reliability of this function has been very useful in establishing the zero time of wave generation or the average depth of propagation in cases where one of these quantities was otherwise unrecorded.

The envelope of waves derived from local disturbances that have been recorded under favorable conditions has usually been well [illegible] in [illegible] cases. Reference 11 shows that this condition [illegible] when either the function of the disturbance or [illegible] derivative are discontinuous. Specific examples given are [illegible] disturbances.

It was found, while using the theory of Reference 11 to compute the dimensions of initial disturbances, that the product of the radius and depth of the disturbance was too small by a factor of $\sqrt{2}$ for energy equivalence with the predicted wave trains. The source of this discrepancy in Reference 11 could not be located. It is felt, however, that because of the agreement of predicted water wall [illegible] the error of $\sqrt{2}$ is confined to the depth of the initial disturbance. (See Appendix B.)

13.3 Underwater Explosion Theory. Two basic concepts of the mode of generation of waves from an underwater explosion have been proposed. One considers the wave to be emitted from a pulsating gas globe that is stationary beneath the surface. Penney (Reference 3, Page 679) considers the initial condition to be the surface disturbance caused by the gas bubble as it vents to atmosphere. The second mechanism finds more favor in the light of experimental evidence.

The energy imparted to the wave train is related to the size of the cavity formed at the surface. For maximum wave-making efficiency, then, Penney's theory requires that the oscillating bubble vents at its maximum expansion phase and, as the oscillations are damped, that it is the first expansion of the bubble that breaches the surface. This places an optimum depth of submergence for the explosion, which is of the order of the radius of the first expansion of the gas bubble.

Assuming the optimum submergence, which he terms the critical submergence, to be equal to the radius of the gas bubble when it reaches the still-water level on the first expansion.

SECRET

the following energy equation is made:

$$4/3\,\pi\, Z_{cr}^3\, \rho g\,(Z_{cr} + a) = (0.40)(W)(3.09)(10^{12}) \qquad (1.2)$$

Where: Z_{cr} = distance below surface, feet; subscript cr denotes critical

ρ = density of sea water

a = atmospheric pressure, feet of water

Forty percent of the yield is assumed to be converted to bubble energy. It is pointed out that this gives fourth-root scaling of Z_{cr} with large yields where the atmospheric head is negligible and cube-root scaling for small charges where Z_{cr} is small compared with a.

For very deeply submerged explosions, the original gas bubble loses its integrity, and multiple venting of smaller bubbles occurs. In the limit, it is conceivable that the bubble, which is presumably steam, will completely condense before reaching the surface, and that surface effects will be the product of intense upwelling of the water in the wake of the rising bubbles. It has been proposed that this situation actually obtained for Wigwam.

Chapter 2

PROCEDURE

2.1 SHOT PREPARATION

Project 1.6 participated in the documentation of the two underwater shots, Wainwo and Umbrella. Wainwo was located about 7,000 feet offshore in about 3,000 feet of water. The device, which yielded about 9 kt, was submerged to a depth of 500 feet. The device for Umbrella was placed on the Eniwetok lagoon floor, which had a general depth of about 150 feet in the vicinity of surface zero. The nearest point of the reef was at a range of about 8,000 feet. The Umbrella yield was about 8 kt.

2.2 PLANNING

Although project planning for the test began in July 1957, delays in the allocation of funds restricted the active building phase to the 4-month period from December 1957 through March 1958.

The building phase involved the development of measurement techniques, assembly and calibration of instrumentation, and choice of station locations. Choice of a particular method of measurement depended upon such factors as the anticipated wave height at range, instrument survival, ease of instrument installation, and ease of record recovery.

Accordingly, the geography of the shot sites was studied, particularly the water depths, reef lines, and available land areas. Station locations were then selected so as to minimize effects of refraction on the propagated wave height and to avoid, where possible, the distortions of the wave record due to reflection from shore and reef lines. In addition, the distribution of available instrumentation was planned to fit in with additional sources of wave data from other projects.

2.3 DATA REQUIREMENTS

To obtain the desired data it was necessary to establish stations at measured ranges and record wave height as a function of time. Alternatively, the wave train could be recorded at a specific instant as a function of range; the nearest practical approach to this was still photography that would show only the locations of crests and troughs and not the amplitudes.

To explore the generative process, it was necessary to have a recording station as near as possible to surface zero and to photograph the development of plume phenomena. For the lagoon shot, before-and-after surveys of the lagoon floor in the vicinity of surface zero were needed.

The computation of wave travel times and refraction paths required that bathymetric and tidal information be available over the area of observation. Time of detonation was to be determinable either from reference to simultaneously recorded events such as air and ground shock or from electric signal.

Evaluation of inundation required the recording of heights reached on shore, together with extent of inundation inland. This was to be correlated with the height attained by the wave crest offshore.

2.4 INSTRUMENTATION

Certain of the instrumentation utilized by the project was similar to that used by the Scripps Institution of Oceanography (SIO) on previous operations. The gyro-inclinometer and the modified Ballistic Research Laboratories (BRL) gage were developed for Operation Hardtack. These two new systems are described in the following sections, as well as certain specialized accessory equipment for use with standard instrumentation. A detailed description of this standard instrumentation can be found in References 4 and 6.

2.4.1 Subsurface Pressure-Time: Modified BRL Gage. Basically, this unit was a differential-pressure recorder connected by a hose to a compliant bladder fixed with reference to the bottom. The system was filled with dry air. This instrument used as its transducing and recording system a standard BRL pressure-time recorder normally used for the measurement of air overpressure. This instrument senses changes in pressure in a metal aneroid-type capsule, which drives a directly coupled stylus that moves on a radius of a battery-driven, chronometrically governed, face-aluminized, glass disk. While the total excursion of the stylus was on the order of 0.050 inch, the trace width was on the order of 0.0005, so satisfactory resolution was obtained with low-power microscopic read-out. Capsules in the 0- to 1-psi range and the 0- to 5-psi range were selected, based on the predicted wave heights.

The BRL gages were modified by changing the internal wiring and by changing the speed of the chart drive motors. Externally, the units were accessorized with a pressure-reserve tank, solenoid-actuated air valves, suitable plumbing, battery power supply, and an electric control circuit programmed by a combination of self-generated signals and the Edgerton, Germeshausen and Grier (EG&G) timing signals. Then the entire recording, pressurizing, and control assembly was packed to be installed in the Navy Radiological Defense Laboratory (NRDL) coracle (a hemispherical welded float, approximately 10 feet in diameter) of Project 2.3 or in the Project 1.6 shells.

The unit was placed in a coracle (or shell) and attached to a preinstalled hose and bladder assembly. During installation of the assembly, the bladder depth was measured exactly by pressurizing the system and noting at what pressure the bladder began to fill. Because accurate volumetric measurements of the entire system were known, the pressure required in the reserve bottle was calculated, so that at equilibrium conditions the bladder was approximately half inflated. At half inflation, the bladder was able to expand and contract sufficiently to compensate for volume changes caused by pressure changes of tide, steric sea level, and the crests and troughs of passing waves. It was about this equilibrium pressure that the differential-pressure capsule operated.

2.4.2 Subsurface Pressure-Time: Wave Recorder, Mark VIII. These units were identical to those used during Operations Castle and Redwing. In essence, the system was a fully temperature-compensated strain-gage absolute pressure transducer connected by a submerged electric cable to a shore-based strip-chart recorder. The transducer was installed in water between 60 and 70 feet deep.

2.4.3 Subsurface Pressure-Time: Turtle Wave Recorder. These units differed only in accessorization from those used with success during Operations Crossroads, Castle, and Redwing. In concept, the units consisted of a bourdon-driven stylus inscribing on a clock-driven anodized-aluminum disk. The entire recorder unit was shock-mounted within a high-pressure steel case. The units were so designed that, by pressurizing or evacuating the inside of the steel case, they could be used in water depths of from 0 to 250 feet. The units were installed in conjunction with a 1,600-pound cast-lead fairing to give them locational stability. The units were accessorized to be started by the arrival of the underwater shock wave, through use of a pressure switch and a solenoid-operated clock-starting device.

Because several locations extremely close to surface zero were necessary, a bourdon-tube protective device was developed, so designed that all pressure signals to the bourdon were

blocked until the arrival of a pressure signal in excess of the ambient value. Receipt of this signal caused a detent to disengage; however, the bourdon was not allowed to receive any signals for about 4 seconds, to allow adequate time for subsidence of extreme initial pressures. Subsequently, the system was open to all pressure signals. Figure 2.1 demonstrates the construction of the protector.

2.4.4 Self-Referencing Wave Recorders: Gyro-Inclinometer. The slope-versus-time curve for a surface station can be integrated to yield the wave height history. If the surface station is a vessel whose length is small compared to the waves of interest and the vessel is oriented bow or stern on the approaching waves, then the pitch angle of the vessel follows the slope of the surface and may be recorded as such. Actually both the pitch angle and the relative heading were recorded so that corrections could be introduced for departures from the end-on attitude.

The sensing element selected for these units was the Minneapolis-Honeywell LABS gyro. As designed, these assemblies were used to feed pitch and roll information to an automatic pilot; however, by rotating one axis through 90°, they were made to aline the contained potentiometers with the pitch and yaw axes. One leg of the pitch potentiometer was combined in a bridge circuit so that the output was amplified and recorded on a standard strip-chart recorder.

One leg of the yaw potentiometer was used as a resistive element in a relaxation, or blocking, oscillator firing a thyratron tube that impressed a marginal dot on the same strip-chart recorder. The oscillating frequency varied as the relative heading of the vessel.

The basic pitch and yaw instrument was accessorized by a battery-inverter power supply and an electronic control system programed by self-generated signals and signals from the EG&G timing circuits. Subsequently, the controller operated in the following manner: Upon receipt of an EG&G signal at H−5 minutes, the inverters and the gyro drive motors were activated. At H−1 minute, the gyro was triggered to uncage on the first hull motion through the horizontal, and the oscillator and chart drive motors were started. At the end of a total run time of 15 minutes, the entire system shut down.

The above combination, as illustrated in Figure 2.2, allowed measurements of pitch to ±30° and yaw to ±60°.

2.4.5 Photographic Measurements of Wave Height versus Time. The Hardtack technical-photography plan revealed that, in several instances, combinations of location, camera size, and lenses gave promise of valuable coverage of target-array vessels and buoys. Such coverage, using standard photogrammetric techniques, could give accurate elevation-versus-time curves for floating objects. It was anticipated that an assortment of data on wave positions, periods, and heights would be derived from analysis of technical photography.

2.4.6 Photographic Measurements of Shoreline Wave Heights. Whenever shorelines suspected of experiencing significant wave action fell within the scope of the technical-photography-plan camera stations, range and elevation poles were installed. Whenever these stations were beyond the range to give adequate coverage of the shoreline area of interest, cameras with timing systems were installed to view these areas.

The contractor-installed 12- by 12-inch wooden poles were painted with alternate horizontal stripes of black and white, 2 feet wide on the vertical dimensions. The poles were set in concrete footings and were guyed wherever required. Photographs of these poles gave data upon the inundation effects of the generated waves.

2.4.7 Visual and Photographic Records by Project Personnel. Wherever possible, project personnel were provided with handheld cameras and stop watches to record wave heights and times of arrival at stations, such as piers projecting into the lagoon, and aboard ships at various ranges from surface zero. Wherever advantageous, striped range poles of suitable caliber were installed on such piers.

2.4.8 Can-Type Inundation Gages. On shorelines expected to receive significant wave action but inaccessible to personnel at shot time, can-type yes-or-no gages were installed at 6-inch increments of elevation to give readings of maximum water depth. Postshot examination for salt water in these cans gave wave elevation on islands and at shorelines. These gages were installed to cover elevations from mean water level to twice the predicted wave height.

2.4.9 Radar Scope Photography. Surface search radar of fleet operational type, when adjusted for high-sea return, could show the range as a function of time of the generated wave crests (Reference 6). Plans were initiated to make these measurements during Shot Wahoo. The scope camera and accessories used for Shot Wigwam were readied.

2.5 TEST-SITE OPERATIONS

2.5.1 Shot Wahoo. Location of Project 1.6 stations and other sources of wave information for Shot Wahoo are shown in Figure 2.3.

It was intended to install BRL gages in five of the Project 2.3 deep-moored coracles. However, the subsurface hose-bladder assembly was damaged upon coracle installation for two of these units, and time was insufficient to effect repair. At shot time, upon receipt of the firing signal, the aneroid capsules for two of the remaining units were ruptured. The record presented by the one BRL gage that operated during Wahoo could not be interpreted.

Mark VIII wave recorders were installed and operated from Sites Elmer and James. The Site James transducer was located just off the reef between Sites Irwin and James and at a water depth of 53 feet. The recording station, which also mounted two project cameras, was carried away by inundating waters from the shot after a partial record had been obtained. The Site Elmer transducer was installed in the lagoon at a water depth of 43 feet.

The cameras mounted on the Site James wave recorder cab were an F-56 and a K-25 aerial camera. They were connected to a common intervalometer and the field of view of the F-56 included a clock. The F-56 was aimed east along the reef, while the K-25 was pointed toward surface zero and the target vessel EC 2. Despite the inundation which completely flooded the lower camera (F-56), the film was salvaged and successfully developed. A range pole was mounted on the reef in the field of view of the F-56 but was carried away by the third wave crest, which crest also claimed the recording station.

Lookout Mountain Laboratories (LML) installed an unmanned 35-mm movie camera on Site Henry (Figure 2.4) and aimed it toward surface zero. The field of view included the DD 592, coracle stations U-4.0 and U-4.6, and wave action on the Henry reef.

Inundation gages were placed on Sites James and Glenn. Those on Site James were washed away, whereas those on Site Glenn were above the level of maximum water rise.

The surface search radar aboard the USS Orlich was adjusted for maximum sea return, and the radarscope was photographed during the event. However, no waves were observed.

A series of before-and-after aerial photographs in both black and white and color were taken of the ocean shoreline from Site Glenn to Site Keith. In addition, a postshot survey gave an approximate record of the maximum water level rise on these islands.

2.5.2 Shot Umbrella. Location of Project 1.6 stations and other sources of wave information for Shot Umbrella are shown in Figure 2.4.

Inasmuch as the turtle wave recorder was expressly designed for close-in recording in shallow water, three of these instruments were installed as close to surface zero as prospects of instrument survival, relocation, and recovery deemed practicable. They were installed in water depths of approximately 160 feet at ranges of from 1,350 to 1,750 feet from surface zero. Although the instrument locations were adequately marked with buoys and all buoys were visible on the day following the shot, the recovery program was delayed by factors beyond the control of project personnel, with the result that all buoys had been destroyed by surface vessels by

D+3 days. One instrument was recovered on D+1 but recovery of the other two turtles was complicated in the extreme in that approximately 400 man-dives were required. The second unit was recovered on D+14 and the remaining unit on D+15.

The gyro-inclinometers installed for Wahoo remained aboard the same vessels for Shot Umbrella. The instrument aboard the DD 474, at a range of 1,930 feet from surface zero, malfunctioned due to an undetermined cause. The instrument on the DD 593 performed satisfactorily.

Two BRL gages were readied to operate in Project 2.3 coracles. On D−1 day, the moorings assigned to these two coracles suffered damage. One was cut free by a surface craft, and the second came adrift. Because the pressure hose to the one had ruptured, that station could not be reactivated. The other station was readied, but the coracle containing the instrument was attached to a mooring that did not have the subsurface pressure sensing assembly.

In addition to the two coracle installations planned for Umbrella, Project 1.6 installed BRL gages in two moored 16-foot fiberglass skiffs. Upon receipt of the firing signal, the aneroid capsule of one of these was ruptured by the automatic pressurizing system. The second operated as expected, but as for Wahoo, the record could not be interpreted.

In addition to the Mark VIII recorder installed off Site Elmer, a Mark VIII station was operated from Site Henry during Umbrella. The transducer was placed in a lagoon water depth of 68 feet and about 3,200 feet offshore.

A K-17 camera was borrowed from Program 9 and mounted on the roof of the instrument cab on Henry. This was operated in conjunction with the project K-25 camera that survived the Wahoo inundation. During the event, both cameras were exposed to a dosage of 105 r, and the lead sheeting, with which they were shielded, was inadequate to prevent fogging.

A photo target buoy was especially placed to be in the field of view of cameras located on Site Henry, but all the film from these cameras was fogged. Photos from other locations indicate that the buoy was obscured by the base surge during passage of the wave train.

Project personnel placed 360 inundation gages along the lagoon shorelines from Site Glenn to Site Keith. Because of the minor extent of the wave action, however, none of the gages were reached by inundating waters.

Project 6.8, which was also interested in subsurface pressure measurements, installed subsurface pressure-time recorders at three stations ranging from 8,300 to 44,800 feet from surface zero. Two of these, Platforms P1 and P3, operated successfully.

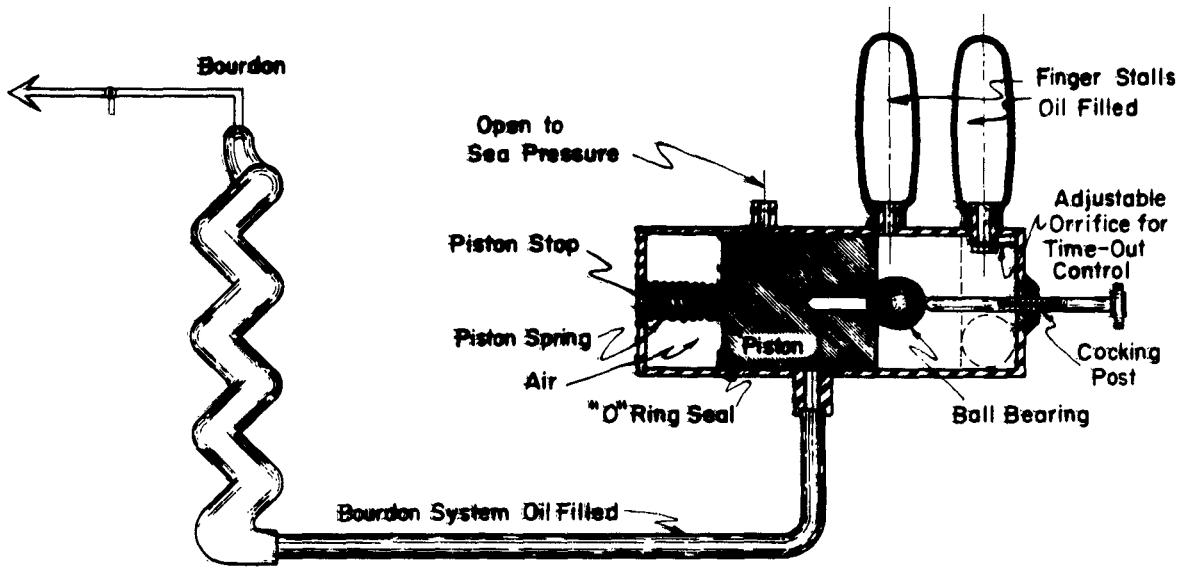

Figure 2.1 Schematic drawing of bourdon protector.

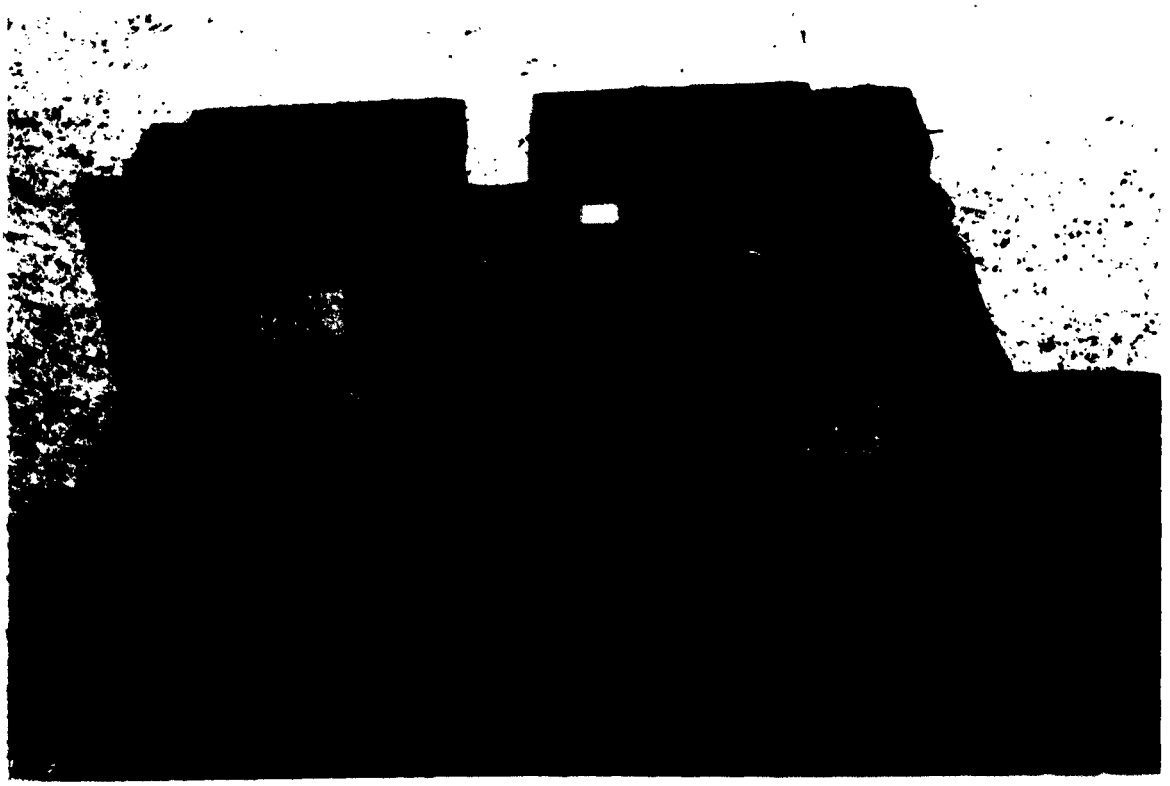

Figure 2.2 Gyro-inclinometer.

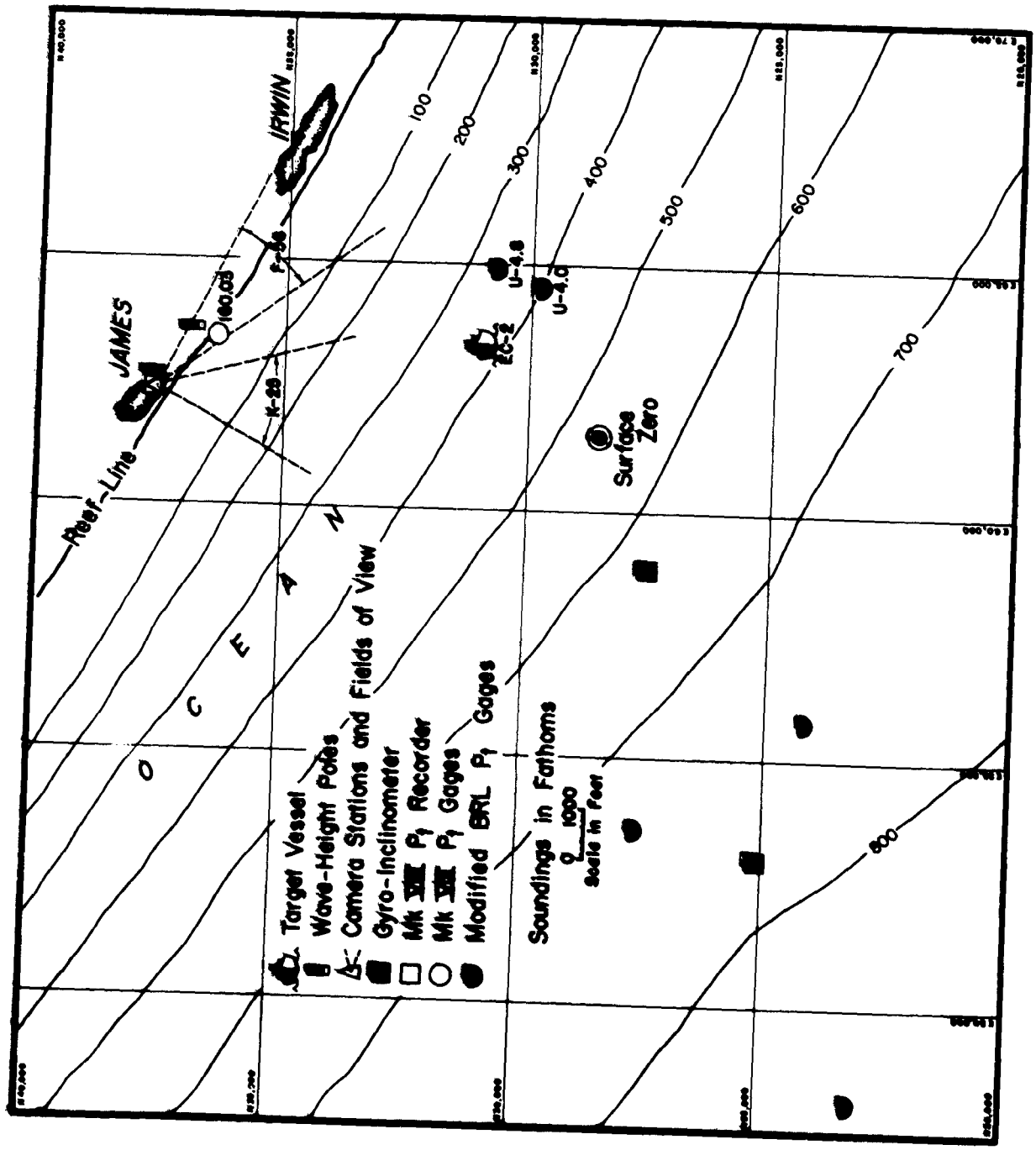

Figure 2.3 Instrument location chart, Shot Wahoo.

Chapter 3

RESULTS

3.1 SHOT WAHOO

3.1.1 Data Obtained. Stations at which wave data was obtained from Shot Wahoo are shown in Figure 2.3. Each observation at a particular location constituted only a partial record for that station.

The closest range at which wave action was observed was that of the target vessel EC 2, 2,500 feet from ground zero. This was a photographic observation by the K-25 camera mounted at Site James and exposing at approximately 2-second intervals. The base surge obscured the vessel soon after passage of the first trough and it did not reappear until after the third trough. A possible node is indicated by the record.

An LML movie camera located on Site Henry viewed wave action at two Project 2.3 coracles, U-4.0 and U-4.8, at surface zero ranges of 3,800 and 4,500 feet, respectively. The length of the target vessel DD 592, oriented broad on in the field of view, was used for calibration. Coracle U-4.0 was enveloped by the base surge after the passage of the first crest, and upon next sighting, the coracle had obviously come adrift and could no longer describe the wave motion at its original station. Coracle U-4.8 was never in the base surge but was periodically obscured by the preceding crests, while in the troughs and after the fourth crest, it was obscured by surf action at the beach. Approximate times of the crest arrivals at the Henry reef could also be measured from the camera record.

The Mark VIII recorder on Site James operated through the fourth crest at which time it was interrupted by the inundating third crest. The recorder was driven off scale by the amplitudes of the third crest, third trough, and fourth crest; however, maximum values were closely estimated from geometric considerations.

3.1.2 Data Reduction. It was necessary to establish the zero time of wave generation, which is hypothesized as the time at which the water crater attains its maximum volume. The available data presented two methods: by observation of timed photographs of surface effects and by analysis of period versus time (dispersion data) from wave records. The dispersion curve depends upon water depth of propagation, range, and time. The dispersion theory of Reference 1 has been shown by References 4 and 5 to reliably define the period-time function. For Wahoo, because of the water depth, over the preponderance of the T – t curve, the Reference 1 dispersion theory coincides with the relationship well established for infinite depth water:

$$T = (4\pi r)/(gt) \tag{3.1}$$

Where: T = period, seconds
t = time, seconds

Uncertainties due to bottom contour are thereby effectively eliminated.

Examination of the periods from the record for which absolute time was most accurately recorded, Station 160.03, indicated that a wave zero time of 9 seconds as referred to shot time would effect the best agreement with dispersion theory.

Photographs of surface effects were studied with a view to estimating the time at which the explosion gases passed through the surface. This appeared to be at about 7 seconds.

Shot time plus 8 seconds was selected as the zero time for purposes of analysis of wave propagation. Times referenced in this report should be so understood unless shot time is specified.

Motion of the Coracles U-4.0 and U-4.8 was transcribed from the film by means of a Vanguard motion analyzer. A smooth curve was constructed through the data. Only the first trough was observed at Coracle U-4.0. Because trough positions of Coracle U-4.8 could not always be observed, the envelope of the wave train was assumed symmetrical about the still-water level, and the troughs were accordingly constructed from the crest envelope. A plot of the wave periods showed a significant departure from theory even after the 8-second correction for zero time had been made. Although the film speed had been nominally 24 frames per second, a speed of 27 frames per second was found to give good agreement between the observed and theoretical periods. Because such a departure in film speed was not considered unreasonable for a camera that had not been intended for technical photography, the wave record was adjusted accordingly. This adjustment also brought the observed wave periods on Henry reef into agreement with dispersion theory.

Observations of wave periods and relative amplitudes on the Henry reef indicate a node in the wave envelope at about 285 seconds. As both the theory of Reference 1 and experimental data of Reference 5 show that this is a feature of a wave that moves at constant velocity from the origin, it was projected back to show the time at which nodes could be expected at Station 160.03 and at U-4.8. The wave envelopes were then constructed through these points and the wave records extrapolated out to the node. The periods of reconstructed waves were ascertained from dispersion theory.

The reconstructed curves are shown in Figure 3.1 together with the partial records from the EC 2, the Coracle U-4.0, and the Henry reef. Reconstructed sections are indicated by broken lines.

The energy content of the first group of waves, which may be considered as containing the preponderance of energy of the train, was calculated from the reconstructed U-4.8 record. In this operation the waveform was considered as sinusoidal and the water depth as infinite. For waves near the front of the train, where the error from the latter assumption might be significant, the wave amplitudes are so low that their contribution to the total energy of the train is insignificant. The energy of the first wave group at 4,500-foot range was 1.3×10^{12} ft-lb. A meaningful measurement of the energy at Station 160.03 cannot be made, because the recorded amplitudes have undoubtedly been influenced by reflection of the wave train from the nearby reef.

The amplitudes shown in the Station 160.03 record of Figure 3.1 have been corrected for the attenuation of subsurface pressure due to water depth and wavelength. Reference 7 was used for this purpose. No reference of the shallow water to deep water wave heights has been made, although this would be desirable to allow a direct comparison between stations. An impulsively generated wave train represents an unsteady-state condition, that is, the flow of energy past any point is not constant but varies roughly as the square of the amplitude envelope. The tables of Reference 7 that relate shallow water to deep water wave height have a constant energy flux as their premise and are therefore not applicable to the transient case.

By way of illustration it can be shown that for the extreme case of referring the height of a wave traveling in very shallow water ($C = \sqrt{gh}$) to its height in deep water. Reference 7 gives

$$\frac{H}{H_o} = \sqrt{\frac{\lambda}{4\pi h}} \qquad (3.2)$$

Where: subscript o denotes the deep water condition
λ = wavelength

It can be shown that this transformation does not conserve the energy of the individual wave; therefore, if the amplitudes of a wave train were adjusted according to Equation 3.2, the resulting figure will not be representative of how the wave train would appear at the same range in deep water, because the total energy will not be the same.

An alternate premise of considering the energy to be conserved within each wave reaches the following conclusion:

$$\frac{H}{H_o} = \sqrt{\frac{\lambda}{2\pi h}} \tag{3.3}$$

A shallow water record referred to deep water by Equation 3.3 will now show the same energy, but the resultant curve still does not represent the wave train after travel to the same range over deep water, because the structure of the train (number of significant waves) has been altered by shoaling.

It appears, then, that any attempt to refer the record of Station 160.03 to deep water would be misleading, and it is, therefore, left as recorded.

It should be noted that the referring of a record from one shallow depth to another shallow depth by the application of Green's law does not result in these inconsistencies. For shallow water both of the afore-considered premises are prevalent. Because the energy is traveling at the phase velocity, there is no dispersion.

3.1.3 Comparison with Other Shots. Other shots which were held in comparable geometries and for which data was available were Shot Wigwam and Shot 147.3C of the Seal series (Reference 2). For each of these the charge was submerged, and the water was sufficiently deep so that the wave train was of oscillatory form without solitary wave characteristics.

3.1.4 Shot Wigwam. The Wigwam data, which, like that from Wahoo, was obtained photographically, was reexamined, and the same reconstruction measures instituted as for the Wahoo coracle record. It was decided that analysis could best be based on the motion of the YFNB 12 at 5,520-foot range. Reconstructed data is shown in Figure 3.2. The dispersion data indicated a wave generation zero time of shot time plus 10 seconds. This coincides with the time observed for the venting of the explosion. Phase zeros, calculated according to Reference 1, were in excellent agreement with those observed for major waves and also disclosed the following point of primary significance: the first trough and crest which were observed by Reference 6 were actually preceded by another full cycle and were, in fact, the second generated trough and crest. The energy of the first trough and crest was dispersed below an observable level and, therefore, could not be detected photographically against the ocean background.

A wave amplitude envelope was judiciously constructed for the first wave group and energy measurement based thereon. The value calculated was 2.65×10^{12} ft-lb, which gives a wave-making efficiency of 3.4 percent. Because this analysis considers more waves than that of Reference 6, the efficiency is accordingly higher.

An amplitude envelope, giving the same node and maximum as that observed, was calculated according to Reference 1. The initial condition assumed was a paraboloidal depression. The dimensions indicated for the crater were a 690-foot radius and a 322-foot depression at the origin. Agreement between the observed and calculated envelopes, as shown by Figure 3.2, was not as good as that for Wahoo.

The observed group velocity, which is the velocity of the maximum of the wave envelope, was 51 ft/sec for Wahoo as compared to 46 ft/sec for Wigwam. According to Reference 1, the group velocities for disturbances of the same geometric type varied directly as the crater radius. The lower group velocity for Wigwam is therefore due to the smaller lateral dimension of its crater despite the fact that the system contained more energy.

It should be borne in mind that the term "crater" might not be entirely applicable to Wigwam, because the great depth of submergence undoubtedly led to a breaking up of the bubble before it reached the surface, as the multiple venting observed at the surface would indicate. Also, condensation of the gas bubble was probably significant in decreasing the potential of the system. This would be compensated in part by induced upwelling of the water surrounding the bubble.

The various papers of Reference 3 point out the complexities encountered in defining the mechanics of an underwater explosion after the first expansion of the gas globe. Calculating

the energy that may be converted to surface waves would seem to be almost a problem in probabilities rather than the application of the usual form of empirical scaling equation. The following derivation, then, should be considered as giving only an indication of what results might be expected from explosions below the lower critical submergence.

The energy contained in a large underwater bubble is directly proportional to its volume and submergence.

$$Q_b = 4/3\ \pi\ R^3\ Z\ \rho\ g \tag{3.4}$$

Where: Q_b = energy, foot pounds; subscript b denotes bubble property
R = radius of generative condition, feet

If the requirement for geometric similarity of submergence of bubbles is $Z \propto R$, then

$$Q_b \propto R^4 \tag{3.5}$$

Assuming the efficiency of bubble formation to be constant with yield;

$$Q_b \propto W \propto R^4 \tag{3.6}$$

The first step in establishing a scaling rule was to explore the variation of wavemaking efficiency, with relative submergence. The function Q_W/W was plotted against $Z/W^{1/4}$ in Figure 3.3 for Wahoo and Wigwam. The line connecting the data showed the relationship.

$$\frac{Q_W}{W} \propto \left(\frac{Z}{W^{1/4}}\right)^{-1/4} \quad \text{or} \quad Q_W \propto \frac{W^{17/16}}{Z^{1/4}} \tag{3.7}$$

Where: subscript W denotes wave train property

Because the objective is to relate this function of Q_W with the maximum wave height observed at any range, an assumption was necessary as to how H varied with r for deep water waves. Lacking indicative experimental data, it was assumed that Hr = constant, which is in agreement with Reference 1. The function of Hr with Q_W was determined by plotting Hr versus $W^{17/16}/Z^{1/4}$ in Figure 3.4.

$$Hr = 1.08\ (10^5)\ W^{17/32}\ Z^{-1/8} \tag{3.8}$$

The nature of the problem and the reliability of the data make it advisable to change the exponent on W to the more convenient $\frac{1}{2}$, in which case the relationship becomes

$$Hr \approx 1.17\ (10^5)\ W^{1/2}\ Z^{-1/8} \tag{3.9}$$

As previously pointed out this formula should not be considered to give more than an indication of what results might be expected from explosions submerged in deep water. It should not be applied to explosions above the lower critical submergence or near the bottom or to small-scale explosions.

3.1.5 Project Seal. Series 147 of Project Seal included the detonation of 4.25-lb TNT charges at varying submergence in a water depth of 13 feet. Reference 2 includes the actual record from one of the shots, 147.3C, which was at the observed lower critical submergence of 4 feet. The record was analyzed from the standpoint of the theory of Reference 1, and energy measurements were made for comparison with Wahoo and Wigwam.

The record from Shot 147.3C consisted of amplitude-time curves at ranges of 50, 126, 172, and 187 feet, plotted simultaneously. The records at the two nearest ranges were undisturbed by reflected waves until their first nodal points, after which time their interpretation became increasingly difficult. The records at 172 and 187 feet were disturbed by reflections even before their first nodes. Because of these disturbances, a theoretical wave envelope was fitted to the nearest record only, and phase zeros were calculated for just the two nearest records.

Of the several initial displacements discussed in Reference 1, the paraboloid yields a wave envelope most like that observed in Shot 147.3C. Thus the calculation of a theoretical envelope

was based on a depression whose radial dimension was chosen so that the theoretical node fitted the observed node. The agreement between the envelopes predicted and observed was not entirely satisfactory, the observed maximum occurring later in the first group than predicted. Also predicted, but not observed, was a bore whose amplitude was approximately half the maximum amplitude of the first group.

The energy of the wave train at 50 feet was found to be 8.25×10^4 ft-lb. Equating this to the energy of a paraboloidal depression, $\pi/6\ \rho\ g\ (R\eta)^2$, where η = amplitude, with R = 11.1 feet as determined from the position of the first node, η = 4.46 feet.

The calculated phase zeros, which are independent of the initial disturbance, were in excellent fit throughout the entire first group at 50 feet, and throughout most of the first group at 126 feet.

To compare Shot 147.3C with Wahoo and Wigwam, the scaling law given by Equation 1.2 was used. Although the atmospheric pressure influences the radius of the bubble formed by a given explosion, the energy that may be transferred to the surface waves from a given size bubble is quite independent of atmospheric pressure. The energy equivalence between the bubble, tangent to the stillwater level, and surface waves, then becomes

$$\epsilon_1\ 4/3\ \pi\ R^4\ \rho\ g\ =\ Q_W \tag{3.10}$$

where ϵ_1 is the efficiency of the process, assumed constant.

The energy of the wave train measured at the closest station was 8.25×10^4 ft-lb. Substituting this value in Equation 3.10 and assuming 100-percent efficiency gives R = 4.21 feet, in good agreement with the actual submergence. This result is highly encouraging, because this particular shot was found experimentally to lie at a critical submergence. Substituting R = 4.21 feet for Z_{cr} in Equation 1.2 and solving for the efficiency of conversion of chemical energy to bubble potential, ϵ_2, gives

$$\epsilon_2\ =\ 11\ \text{percent} \tag{3.11}$$

An energy equivalence of 1.5×10^6 ft-lb/lb of explosive was used. The charge contained 2 ounces of primer in addition to $4\frac{1}{4}$ pounds of TNT, so the weight of explosive was 4.38 pounds. The efficiency calculated above compares with the value of 40 percent assumed in Reference 3. It must be observed that ϵ_2 includes approximately $(\epsilon_1)^{3/4}$, but this value should be much nearer to unity than the observed discrepancy would indicate.

Figure 3.5 was constructed on the form of Equation 1.2, using the above-derived efficiency of 11 percent, and it scales the lower critical submergence observed for Seal up to the yields of Wahoo and Wigwam. The datum points plotted for the two nuclear shots indicate that their submergence was below the lower critical; therefore, the radii of the bubbles reaching the surface were well below the maximum possible for their yields. The transition from cube root to fourth root scaling is illustrated by Figure 3.5, the asymptotes of the equation being plotted.

No account has been taken here of the probable inequivalence of effects between chemical and nuclear explosions.

3.1.6 Inundation Data. Inundation data for Wahoo was obtained by a postshot survey, which noted the heights reached by water and extent of penetration inland. These observations together with selected photos of inundation effects are contained in Appendix A. Sites Irwin and James were completely inundated. The heights to which debris was noted to be lodged in trees were as great as 15 feet. Runup on adjacent islands was 5 to 9 feet above tide stage.

Reference 4 observed that the breaker height at the beach was approximately 2.5 times the crest height recorded in 60 feet of water offshore. The James recorder showed a maximum crest height of 9.3 feet in 53-foot water depth. This represents a breaker height of about 23 feet, which agrees well with the observed inundation levels on the island.

3.2 SHOT UMBRELLA

3.2.1 Data Obtained. Stations at which data was obtained from Shot Umbrella are shown in

Figure 2.4. Usable records were from the three turtles, the DD 593 gyro-inclinometer, Sites Henry and Elmer Mark VIII stations, and from Project 6.8 Platforms P1 and P3.

3.2.2 Data Reduction. All subsurface pressure-time records were corrected for the attenuation due to instrument depth and wavelength. This correction itself introduces a certain amount of distortion into the record wherever the rate of change of period is great. This occurs at the first crest and at envelope nodes where the phase reverses. Corrected records from the three turtles and Platform P1 are shown in Figure 3.6.

The slope record from the gyro-inclinometer was numerically integrated to give a surface displacement record. Here a drifting base line in the original record complicated the problem. A new base line was established by arbitrary means prior to integration. Because the form of the displacement curve is highly sensitive to the particular base line established, the record can only be evaluated for period and an indication of maximum wave height.

The energy for the wave train was calculated, assuming radial symmetry and shallow water velocity (Table 3.1). Records of shallow water explosions always commence with a crest that arrives at a station at a time earlier than that predicted for a shallow water wave or even for a solitary wave if calculated from the origin at zero time. Reference 4 concludes that this first crest is the result of a water crater lip that is already advanced in range at the time taken as zero for wave generation. As the shallow water depth results in very little energy dispersion, energy of the remainder of the train following the first crest is considered equivalent to the potential energy of the water crater. Taking energy measurements at the closest range station, the dimensions of a water crater can then be calculated. For very shallow water, the assumption that a cylindrical cavity extends to the lagoon floor is as good an approximation as any and enjoys the advantage of simplicity. Table 3.1 also shows crater radii calculated from the three turtle records. This is plotted versus yield in Figure 3.7, together with data from other nuclear explosions. It is seen that the Umbrella crater radius is very near the extrapolated curve for the Redwing surface shots, in contrast to other submerged shots that fall well above this line.

As the Redwing results showed $W^{1/2} h_g^2$ to be directly proportional to the wave energy for surface shots, this function was also plotted as Figure 3.8, and the Umbrella data again coincided with the surface shot data. A scaling law was then derived for surface explosions, using the Umbrella data to extend the curve to lower yields.

Wave height versus range data was plotted in Figure 3.9 for well-documented lagoon shots. The maximum crest height was used and referred to the depth of generation by Green's law. It is necessary that the reference depth be a generation parameter rather than an arbitrary value, in order to allow comparison between shots fired in various depths. For each shot, a line was drawn defining $H_c r^n$ as constant. The exponent, n, varied from shot to shot but the average value was 0.86. $H_c r^{0.86}$ was assumed to be a function of Q and was therefore plotted versus $W^{1/2} h_g^2$ in Figure 3.10. Each datum point in this figure represents an observation at a particular station for a particular shot. The scaling equation derived from Figure 3.10 was

$$H_c r^{0.86} = 25\, h_g W^{1/4} \tag{3.12}$$

As for previous scaling equations, caution should be exercised in applying it to conditions outside the range of data from which it was derived. Especially, as the ratio of crater radius to water depth becomes less, the approximation of a cylindrical initial depression becomes less valid.

Figure 2.4. Usable records were from the three turtles, the DD 593 gyro-inclinometer, Sites Henry and Elmer Mark VIII stations, and from Project 6.8 Platforms P1 and P3.

3.2.2 Data Reduction. All subsurface pressure-time records were corrected for the attenuation due to instrument depth and wavelength. This correction itself introduces a certain amount of distortion into the record wherever the rate of change of period is great. This occurs at the first crest and at envelope nodes where the phase reverses. Corrected records from the three turtles and Platform P1 are shown in Figure 3.6.

The slope record from the gyro-inclinometer was numerically integrated to give a surface displacement record. Here a drifting base line in the original record complicated the problem. A new base line was established by arbitrary means prior to integration. Because the form of the displacement curve is highly sensitive to the particular base line established, the record can only be evaluated for period and an indication of maximum wave height.

The energy for the wave train was calculated, assuming radial symmetry and shallow water velocity (Table 3.1). Records of shallow water explosions always commence with a crest that arrives at a station at a time earlier than that predicted for a shallow water wave or even for a solitary wave if calculated from the origin at zero time. Reference 4 concludes that this first crest is the result of a water crater lip that is already advanced in range at the time taken as zero for wave generation. As the shallow water depth results in very little energy dispersion, energy of the remainder of the train following the first crest is considered equivalent to the potential energy of the water crater. Taking energy measurements at the closest range station, the dimensions of a water crater can then be calculated. For very shallow water, the assumption that a cylindrical cavity extends to the lagoon floor is as good an approximation as any and enjoys the advantage of simplicity. Table 3.1 also shows crater radii calculated from the three turtle records. This is plotted versus yield in Figure 3.7, together with data from other nuclear explosions. It is seen that the Umbrella crater radius is very near the extrapolated curve for the Redwing surface shots, in contrast to other submerged shots that fall well above this line.

As the Redwing results showed $W^{1/2} h_g^2$ to be directly proportional to the wave energy for surface shots, this function was also plotted as Figure 3.8, and the Umbrella data again coincided with the surface shot data. A scaling law was then derived for surface explosions, using the Umbrella data to extend the curve to lower yields.

Wave height versus range data was plotted in Figure 3.9 for well-documented lagoon shots. The maximum crest height was used and referred to the depth of generation by Green's law. It is necessary that the reference depth be a generation parameter rather than an arbitrary value, in order to allow comparison between shots fired in various depths. For each shot, a line was drawn defining $H_c r^n$ as constant. The exponent, n, varied from shot to shot but the average value was 0.86. $H_c r^{0.86}$ was assumed to be a function of Q and was therefore plotted versus $W^{1/2} h_g^2$ in Figure 3.10. Each datum point in this figure represents an observation at a particular station for a particular shot. The scaling equation derived from Figure 3.10 was

$$H_c r^{0.86} = 25\, h_g W^{1/4} \tag{3.12}$$

As for previous scaling equations, caution should be exercised in applying it to conditions outside the range of data from which it was derived. Especially, as the ratio of crater radius to water depth becomes less, the approximation of a cylindrical initial depression becomes less valid.

TABLE 3.1 WAVE DATA, SHOT UMBRELLA

Station	Range	Wave Energy, Total	Wave Energy, Excluding First Crest	Radius of Cylindrical Crater
	ft	ft-lb	ft-lb	ft
163.01	1,700	13.2×10^{10}	7.6×10^{10}	187
163.02	1,350	13.5×10^{10}	10.0×10^{10}	215
163.03	1,750	12.0×10^{10}	7.3×10^{10}	184
Project 6.8				
Platform 1	8,300	7.4×10^{10}	6.3×10^{10}	*
Platform 3	44,700	8.8×10^{10}	8.5×10^{10}	*

* Not applicable because of energy dispersion.

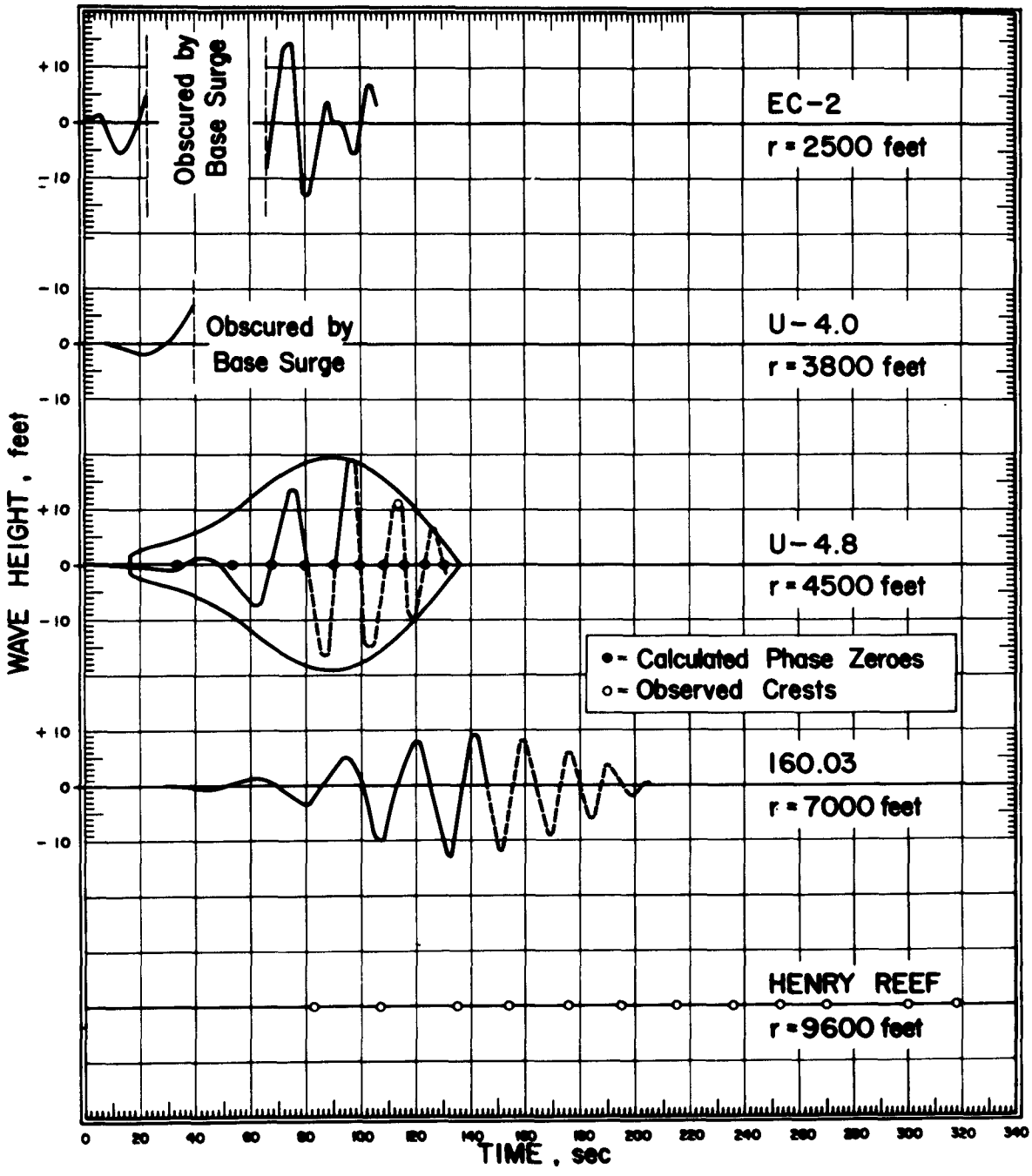

Figure 3.1 Wave records, Shot Wahoo. Wave crests on Henry reef were observed as the wave broke. Note that only a single point was observed for the fourth crest at U-4.8. The dashed portions of the curve were not observed but were constructed from theoretical considerations. Absolute values for amplitudes on Henry reef could not be ascertained.

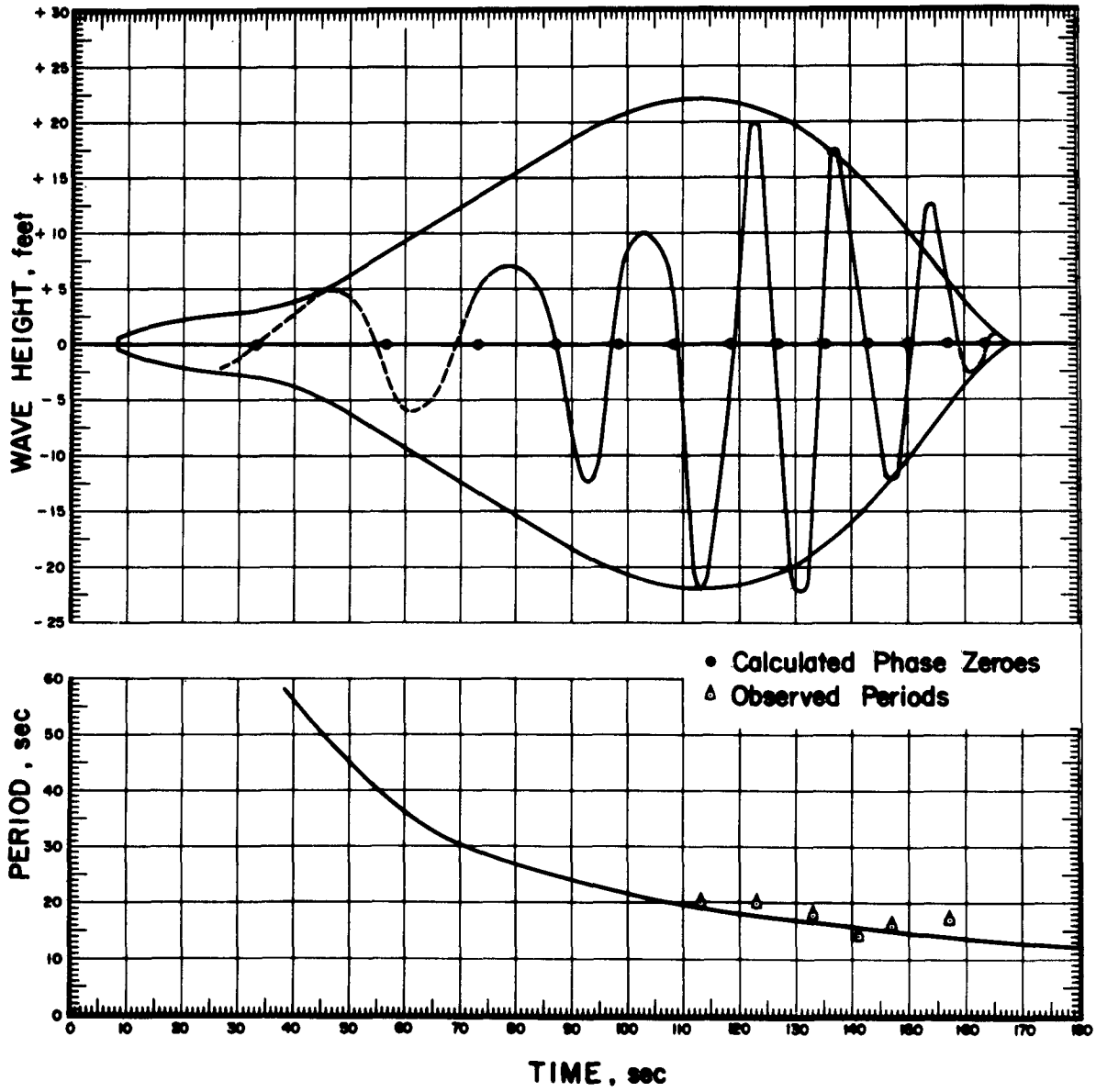

Figure 3.2 Wave record from YFNB 12, Shot Wigwam. Dispersion curve measured from shot time. Wave height curve measured from shot time plus 10 seconds. Reconstructed sections shown as dashed lines.

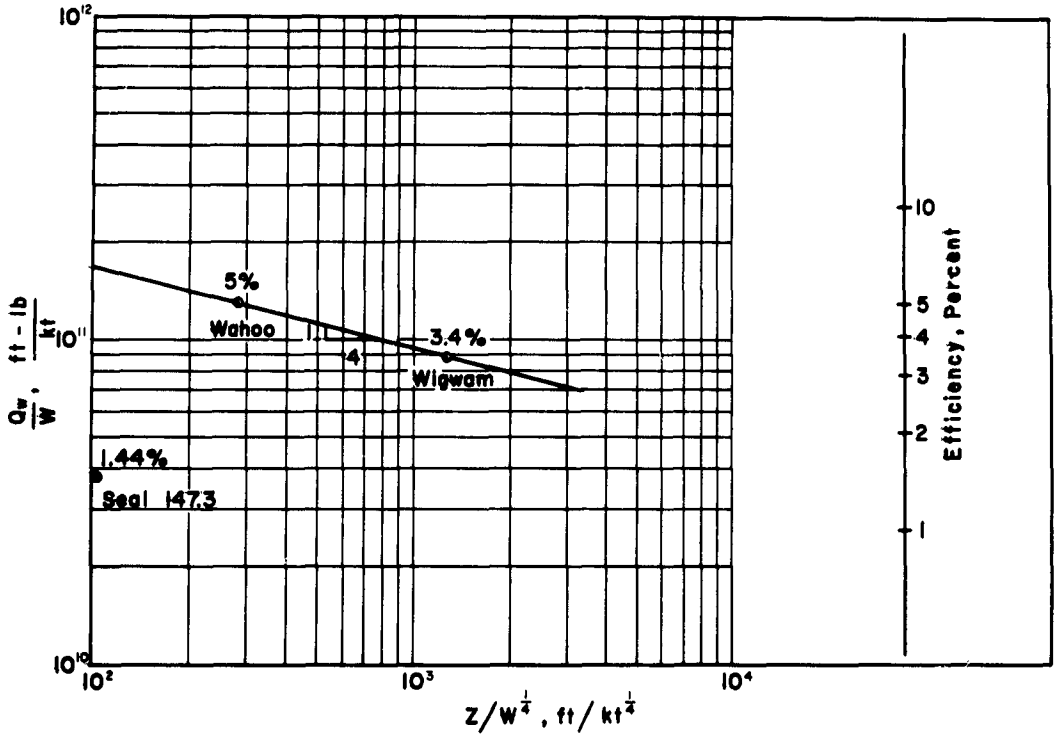

Figure 3.3 Graph of Q_w/W versus $Z/W^{1/4}$. Efficiency based on 2.6×10^{12} ft-lb/kt.

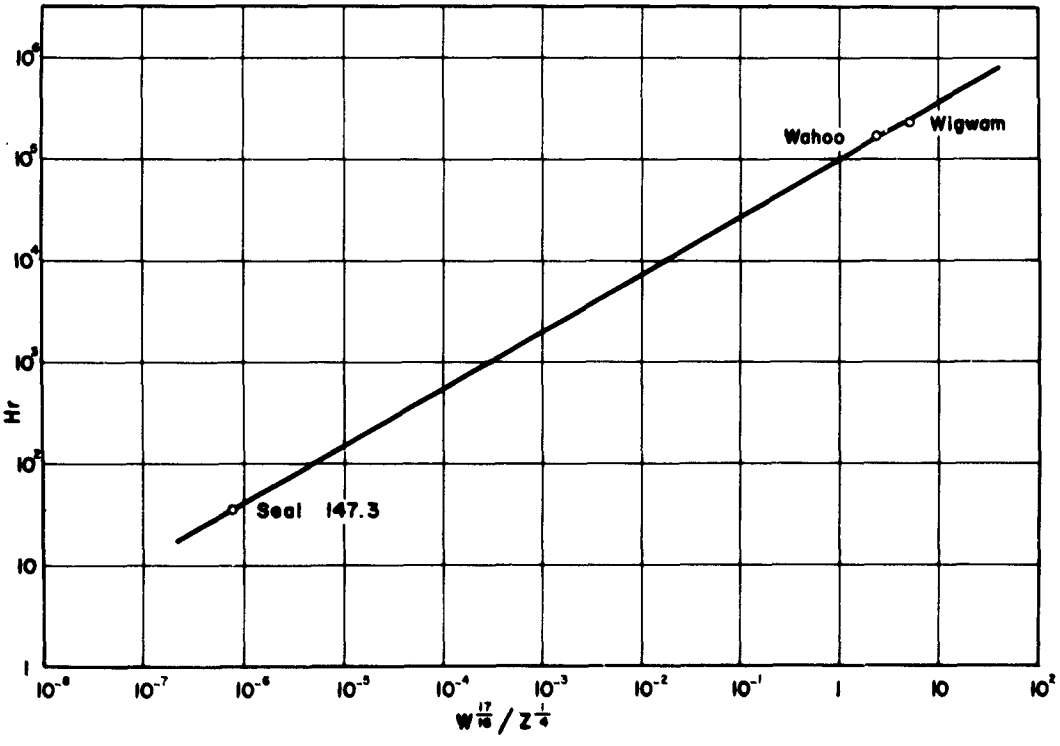

Figure 3.4 Graph of Hr versus $W^{17/16}/Z^{1/4}$. Slope of line is 0.57.

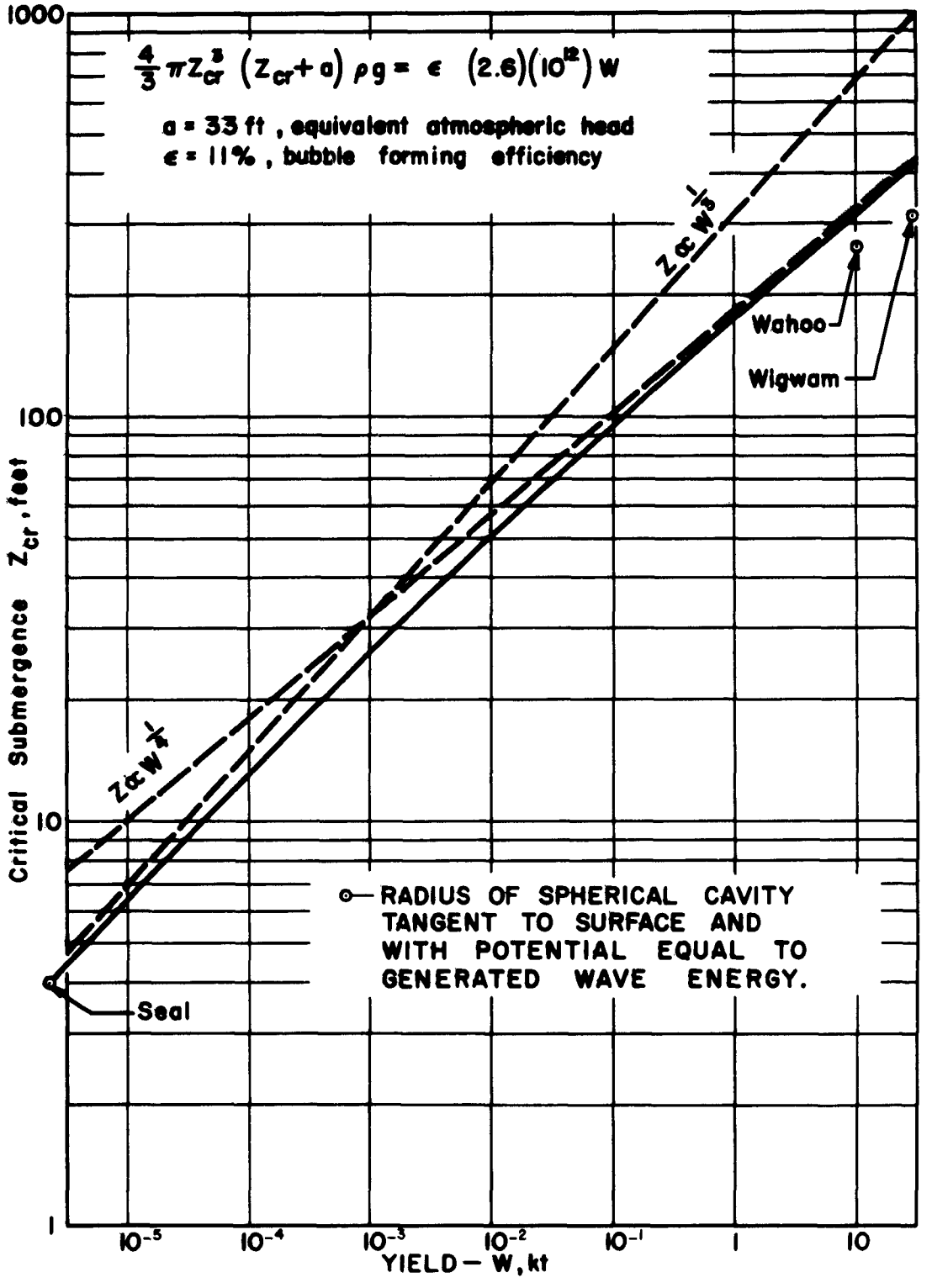

Figure 3.5 Graph of Z_{cr} versus yield. Seal data converted from fresh to sea water.

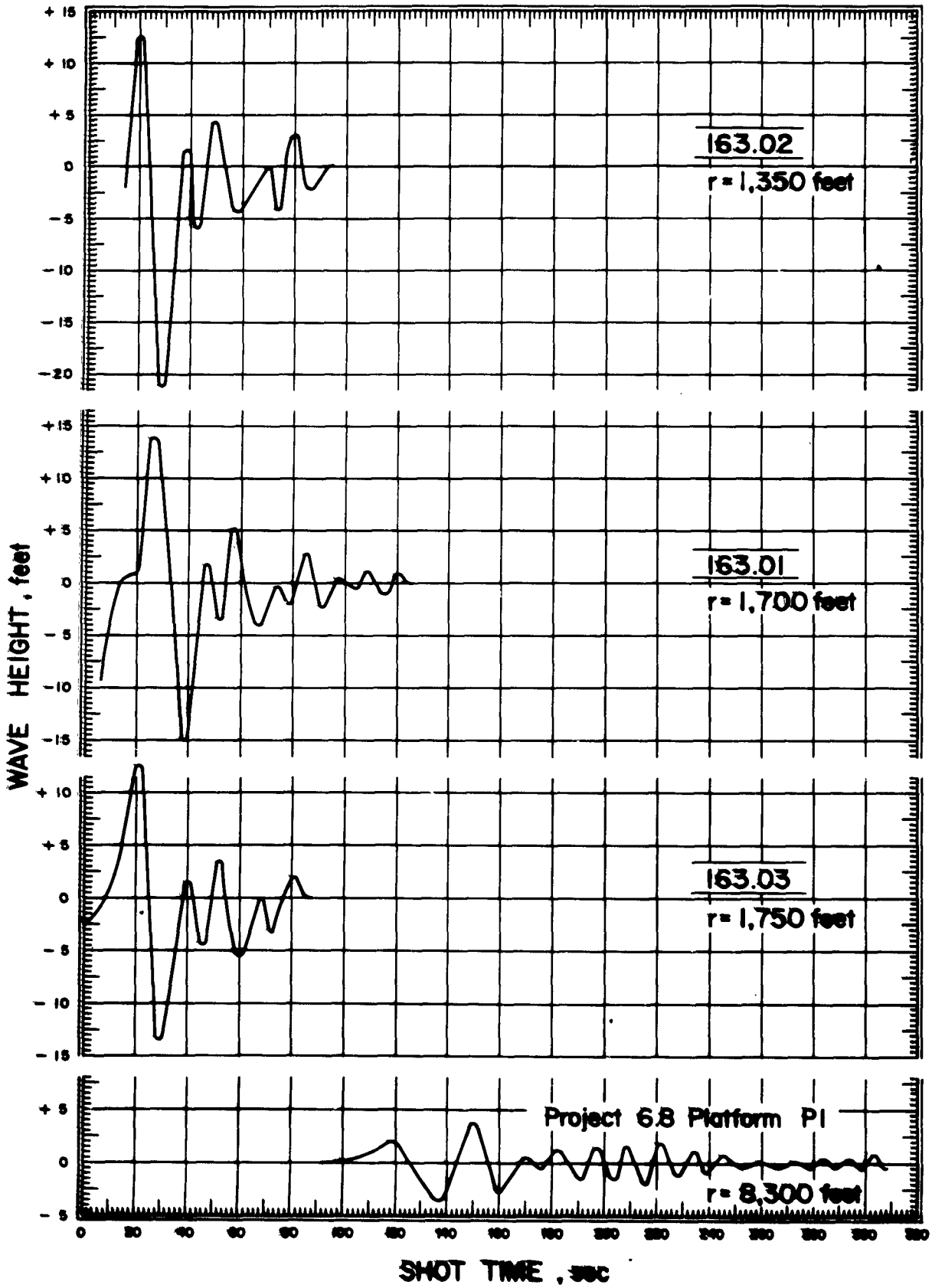

Figure 3.6 Wave records, Shot Umbrella.

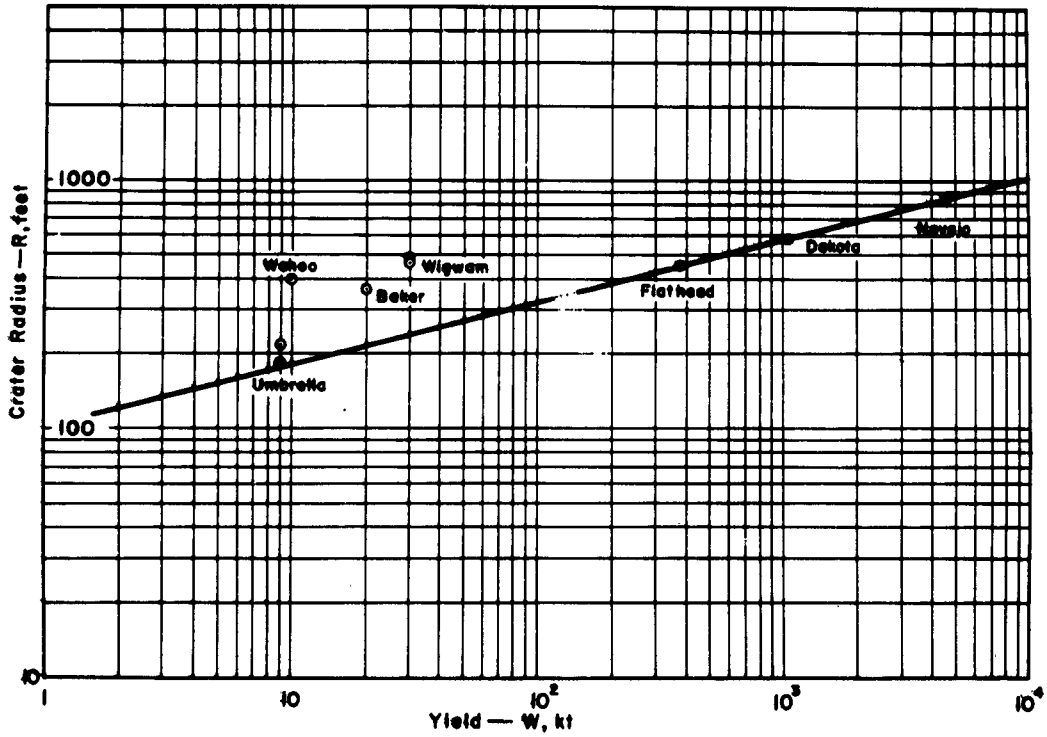

Figure 3.7 Graph of crater radius versus yield. Equation of line is $R \propto W^{1/4}$.

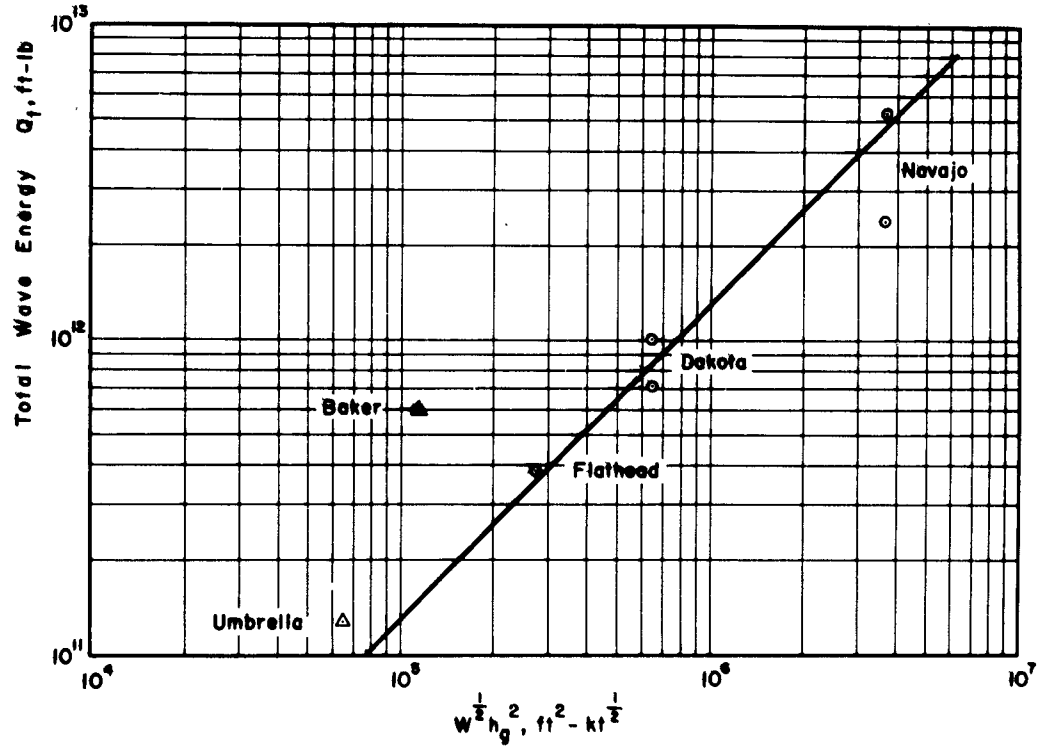

Figure 3.8 Graph of Q_T versus $W^{1/2} h_g^2$. Equation of line is $Q_T = 1.3 \times 10^6 W^{1/2} h_g^2$ ft-lb.

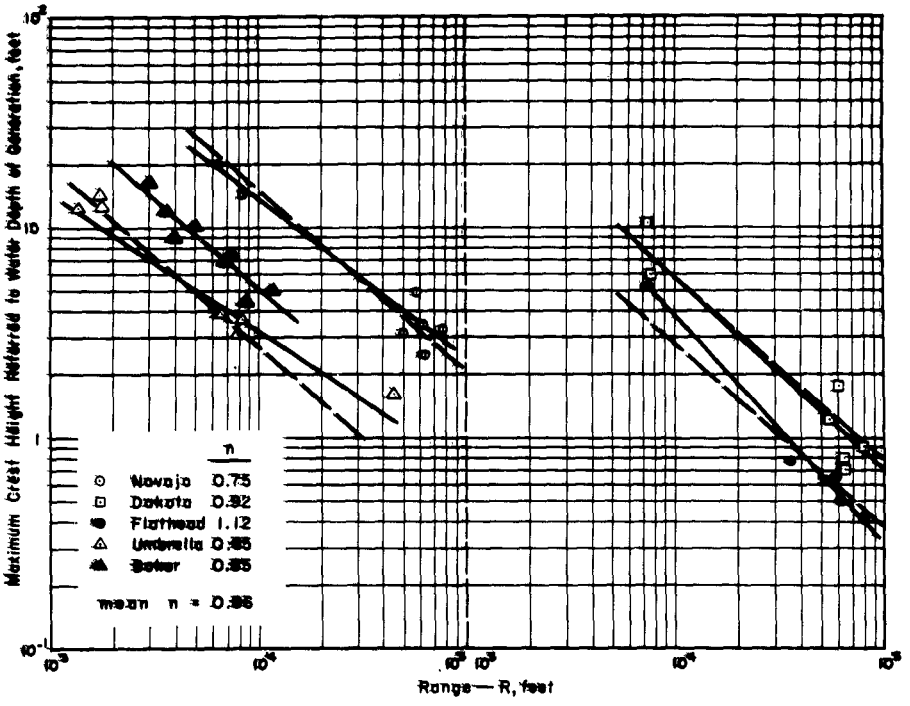

Figure 3.9 Graph of H referred to depth of generation versus r, in two sections to insure clarity. Equations of lines are of the form $H_c \propto r^n$. Equation of dashed line is $H_c \propto r^{0.86}$.

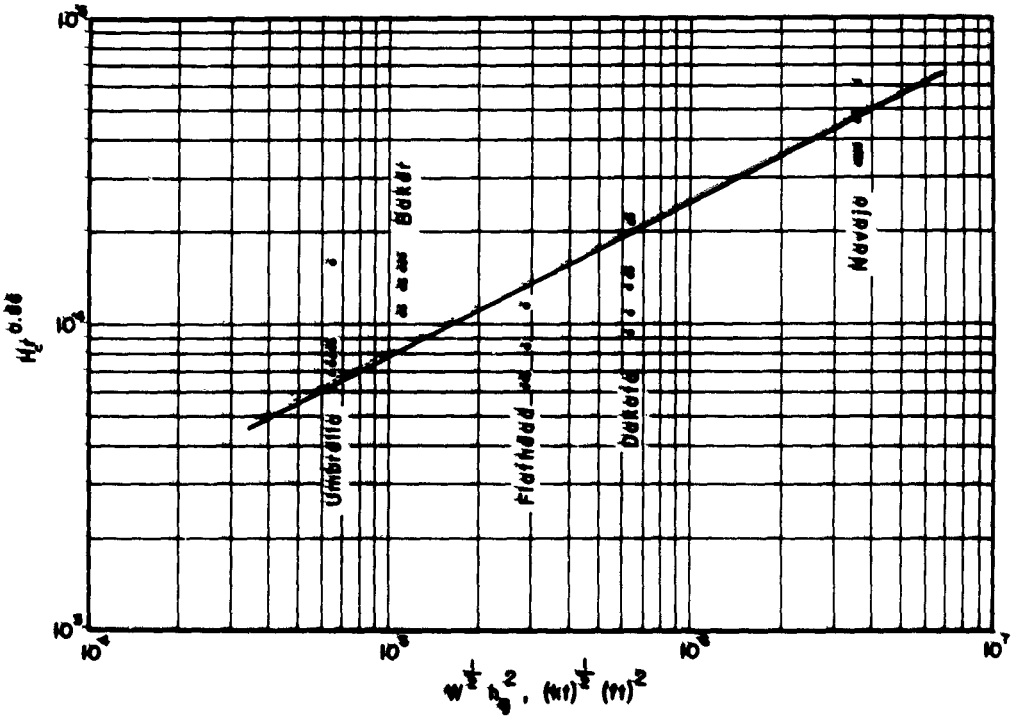

Figure 3.10 Graph of $H_c r^{0.86}$ versus $W^{1/2} h_g^2$. Equation of line is $H_c r^{0.86} = 25\, W^{1/4} h_g$.

Chapter 4

CONCLUSIONS AND RECOMMENDATIONS

4.1 CONCLUSIONS

Study of Wahoo waves and other deep water wave trains has indicated an area of agreement between the theory of Reference 1 and observation. The amplitude envelopes could be approximately described by paraboloidal source conditions whose dimensions were of the same order as those observed photographically. The primary uncertainty is in the factors determining the aspect ratio of the initial disturbance.

The complex mechanics of underwater gas globes indicate that the derivation of a wave scaling law for bubbles that vent at a time much greater than the first expansion is perhaps unrealistic. However, perhaps a formula based on past observation will indicate the order of magnitude to be expected. Experiments with detonations venting upon or before the first expansion of the gas globe should meet with successful empirical analysis.

Examination of model laws has indicated the feasibility of exploring the generation parameters on a much smaller scale than Wahoo and Wigwam. Although the transition from cube to fourth power scaling of bubble energy with yield has been defined in Reference 3, it does not seem to have been given much regard by students of explosion waves. Ignorance of this function of atmospheric pressure has led to gross errors in previous attempts at scaling from small chemical explosions.

The height reached by inundating Wahoo waves on Site James was in the same ratio to the offshore crest as that observed during Operation Redwing. Scaling of shallow water wave height from deep water explosions, however, presents a complex problem.

The waves generated by Umbrella were not significantly different from what would have been expected from a surface explosion of the same yield. Because all other submerged shots have exhibited a marked increase of wavemaking efficiency over that for a surface shot, it must be concluded that the proximity of Umbrella to the bottom was the unique circumstance that made it the exception. Inclusion of the Umbrella data with that of Redwing surface shots has led to a scaling formula of perhaps wider applicability.

The extent of penetration inland of inundation waters was inconclusive. Those islands directly hit were totally inundated. Those only partially inundated were situated so that their beaches were at a small angle to the bearing to surface zero. The impinging waves underwent considerable refraction and consequent energy dispersion.

4.2 RECOMMENDATIONS

The effort in future tests should be concentrated on direct measurement of generative parameters as well as generated phenomena. Measurement of crater dimensions in deep water explosions could perhaps be accomplished by sonar systems. The feasibility of such sonar instrumentation should be studied. Examination of bottom cores from shallow water explosions would probably yield valuable information regarding the crater shape before wash-back of material during water crater collapse. The proximity to surface zero at which waves are recorded must be pushed to the limit.

Instrument development must stay abreast of documentary requirements. The insufficient allotment of time for this purpose, which extended contract negotiations have imposed upon the past operation, must not hamper future programs. Otherwise, compromise of the objectives will again be the inevitable result.

Appendix A

INUNDATION DATA

Included in this appendix are charts of Sites Glenn, Henry, Irwin, James, and Keith, showing the extent of inundation from Shot Wahoo, and the movement of large objects due to this inundation. Also included are selected pre- and post-Wahoo comparison photographs of Sites Henry, Irwin, James, and Keith, and photographs of the arrival of the first three Wahoo crests at the James-Irwin reef.

Inundated areas are shown on the charts by hatching. On these charts the island boundary is given by the high tide line, which is 5 feet above a datum approximately ½ foot below mean low water springs.

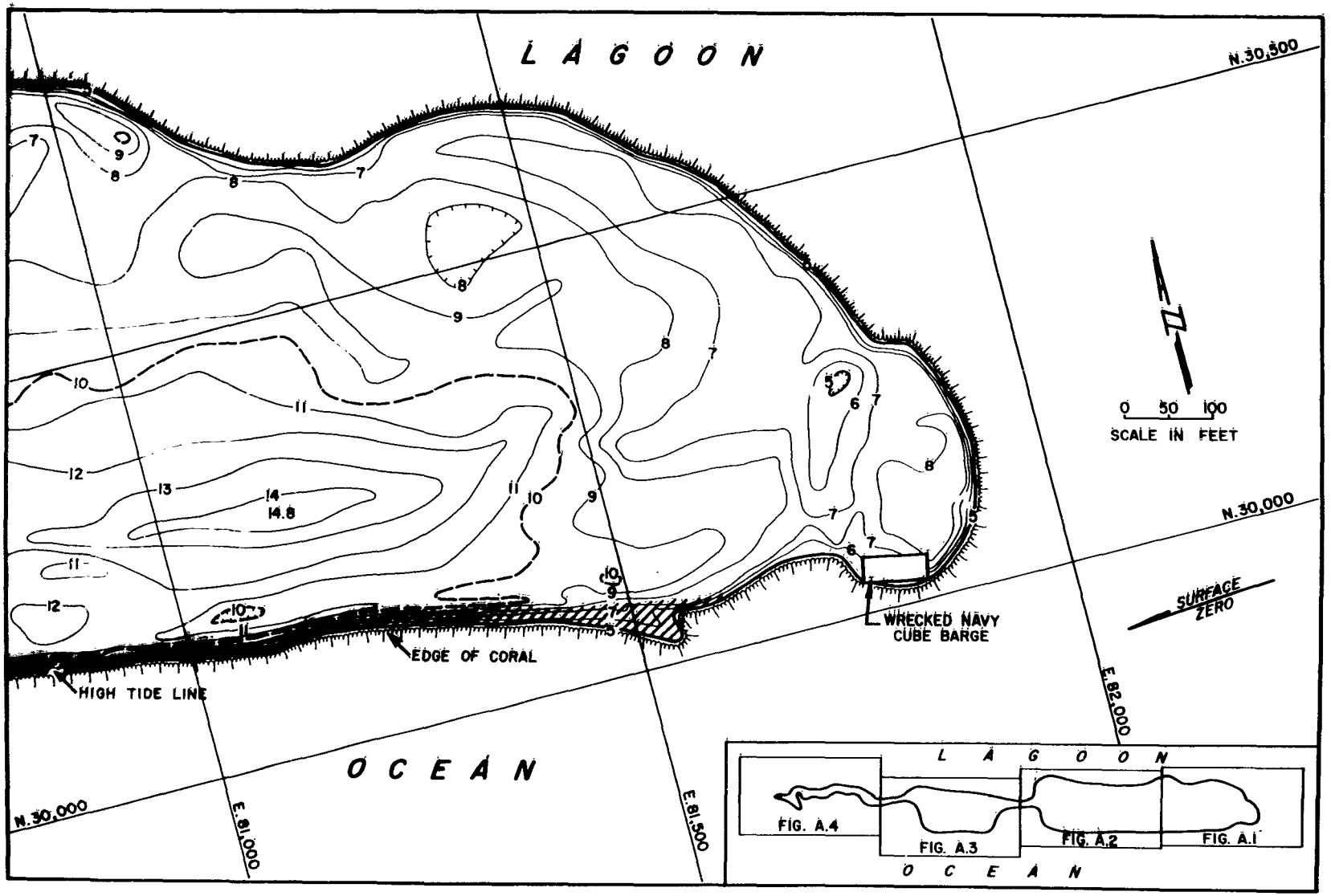

Figure A.1 Wahoo inundation chart: Glenn. Entire area of island in this figure dense with brush and palm trees.

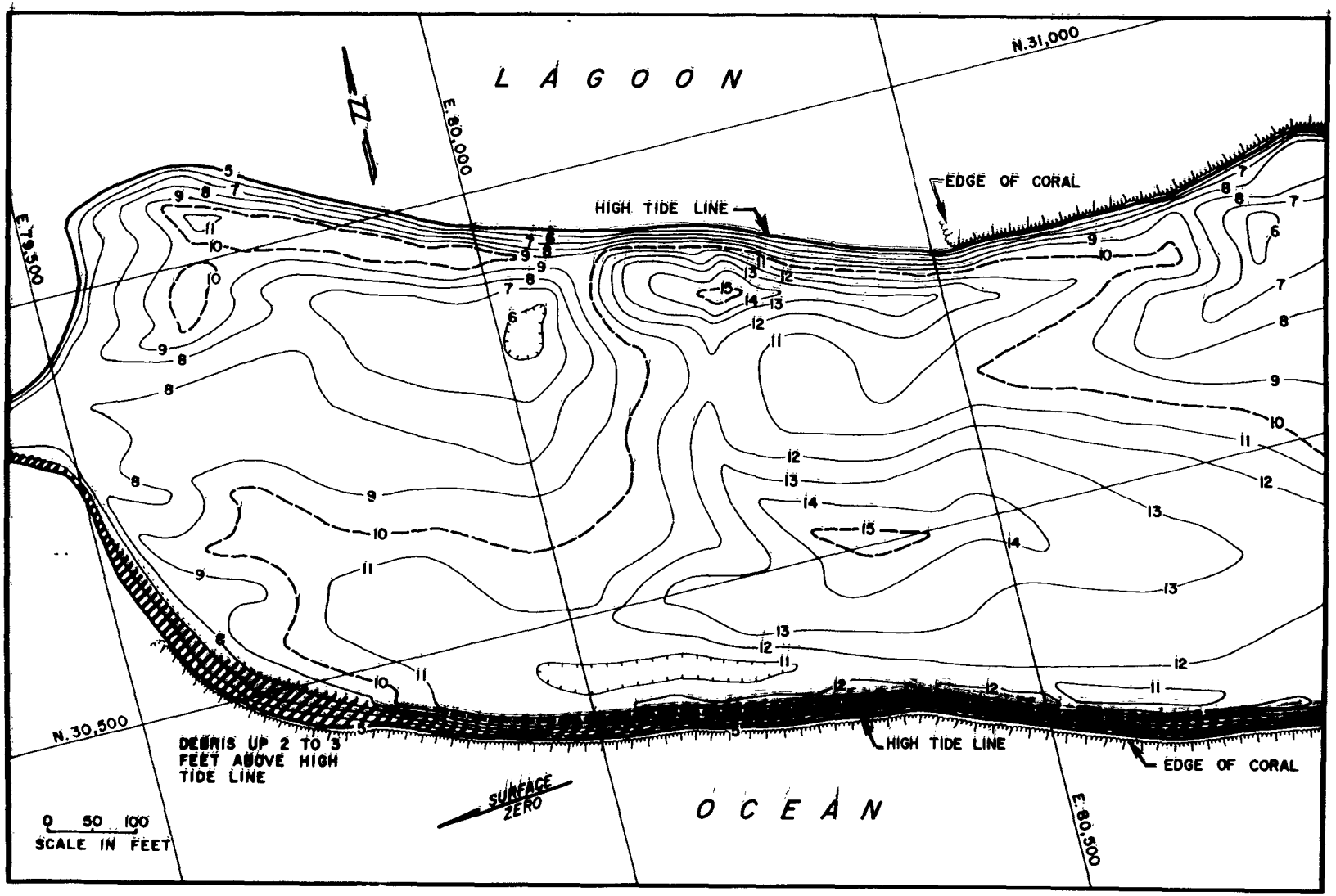

Figure A.2 Wahoo inundation chart: Glenn. Entire area of island in this figure dense with brush and palm trees.

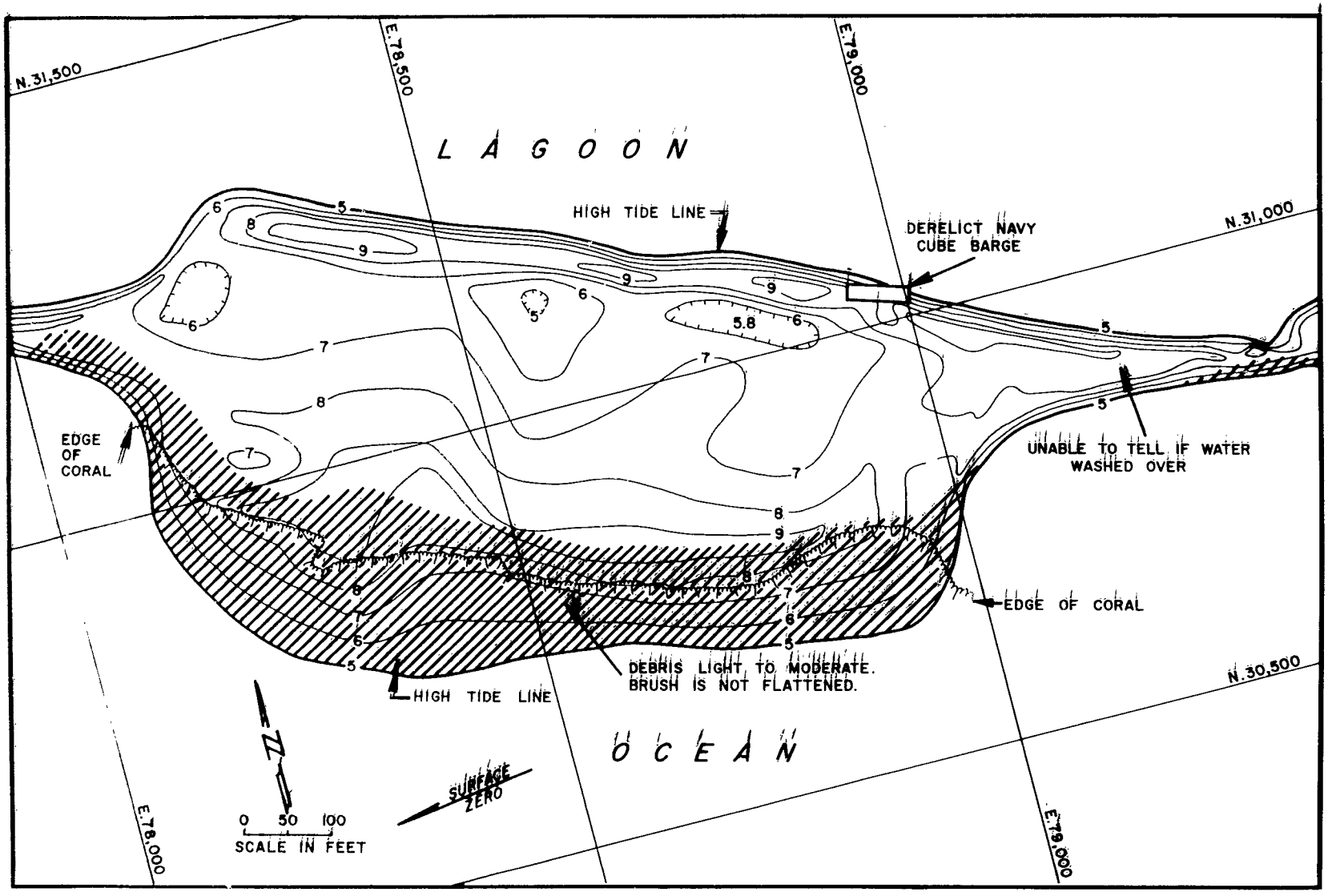

Figure A.3 Wahoo inundation chart: Glenn. Entire area of island in this figure dense with brush and palm trees.

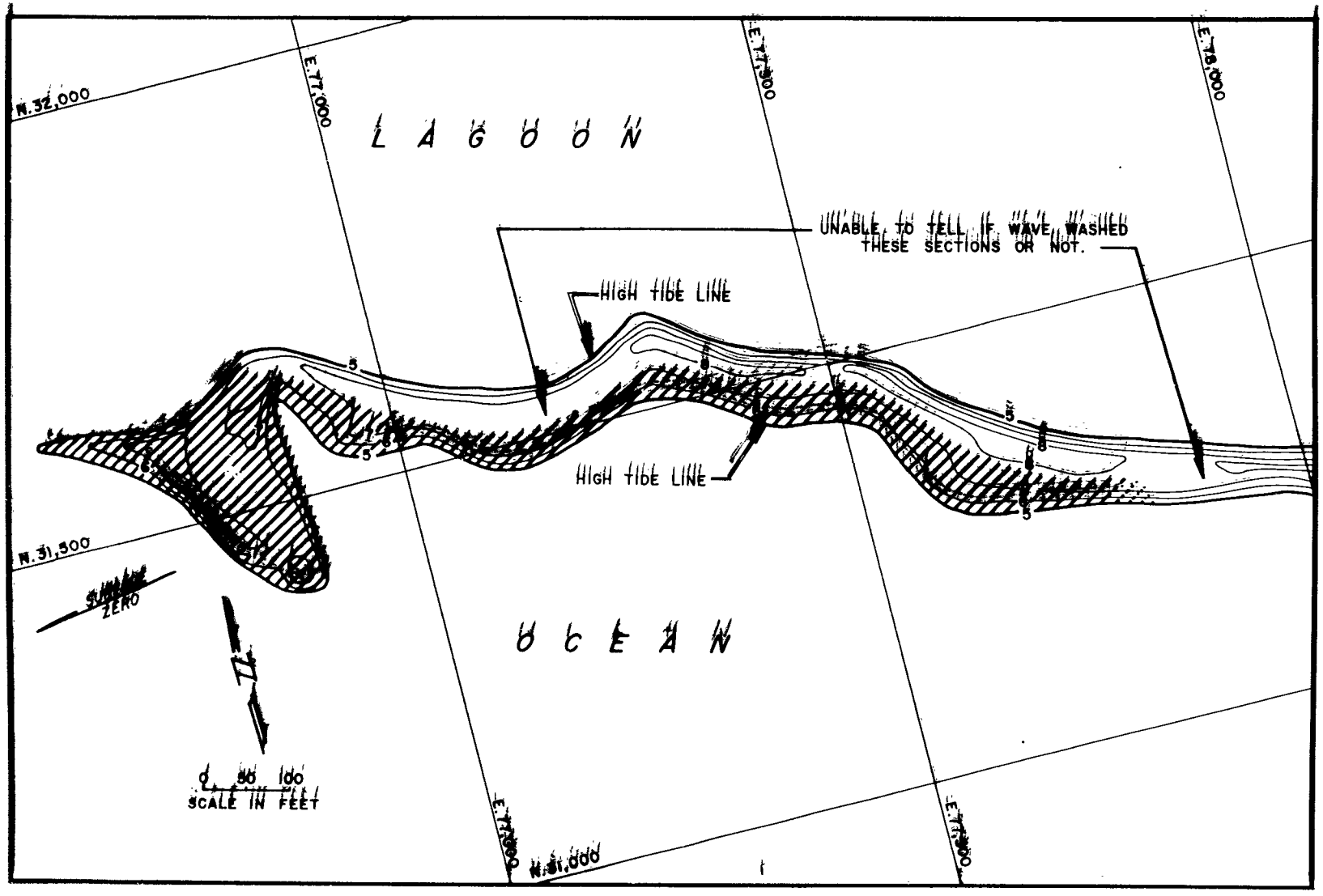

Figure A.4 Wahoo inundation chart: Glenn. The area of Glenn in this figure a sand bar with scattered brush along higher points.

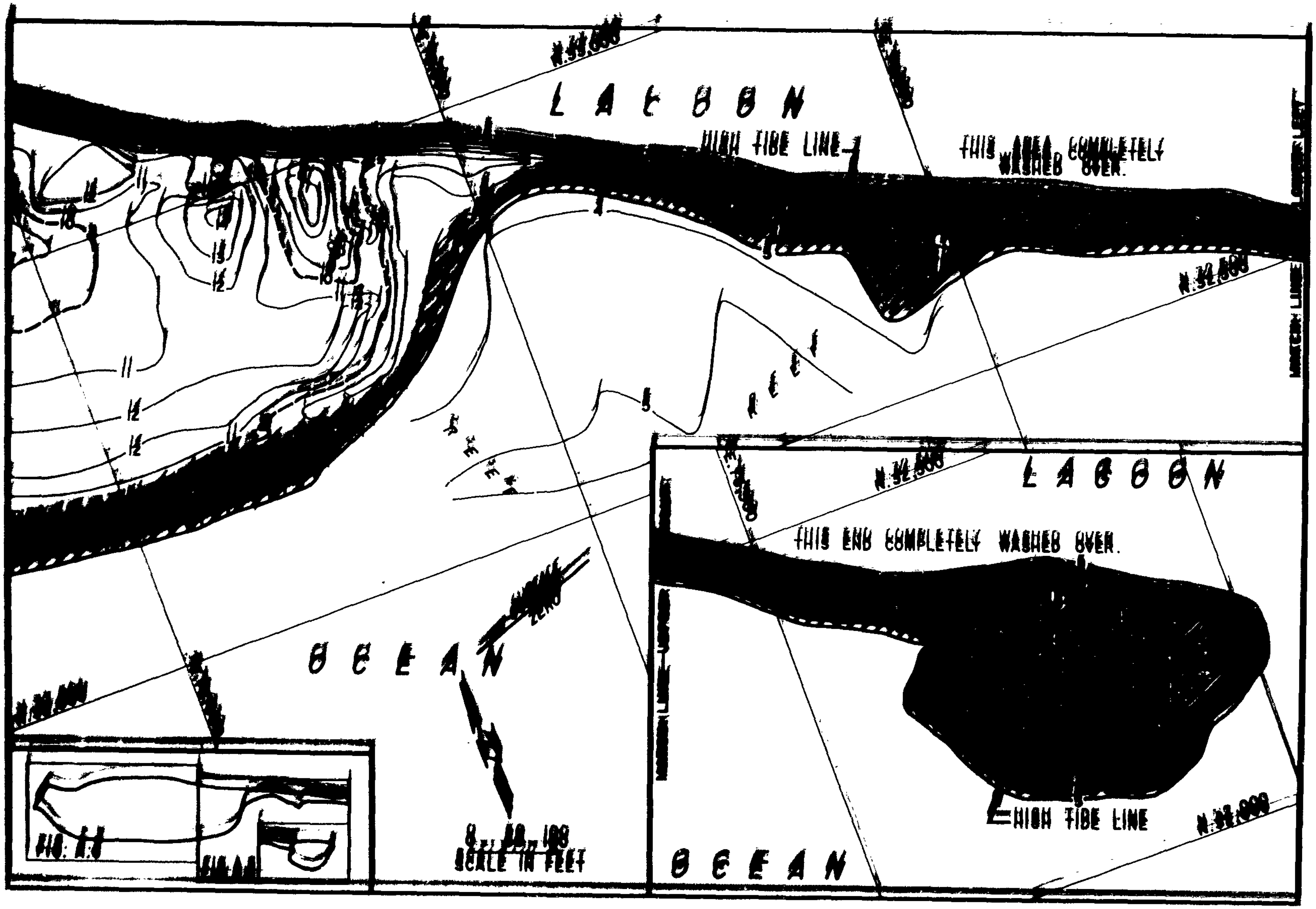

Figure A.5 Wahoo inundation chart: Henry. Entire island beach sandy except where noted as coral.

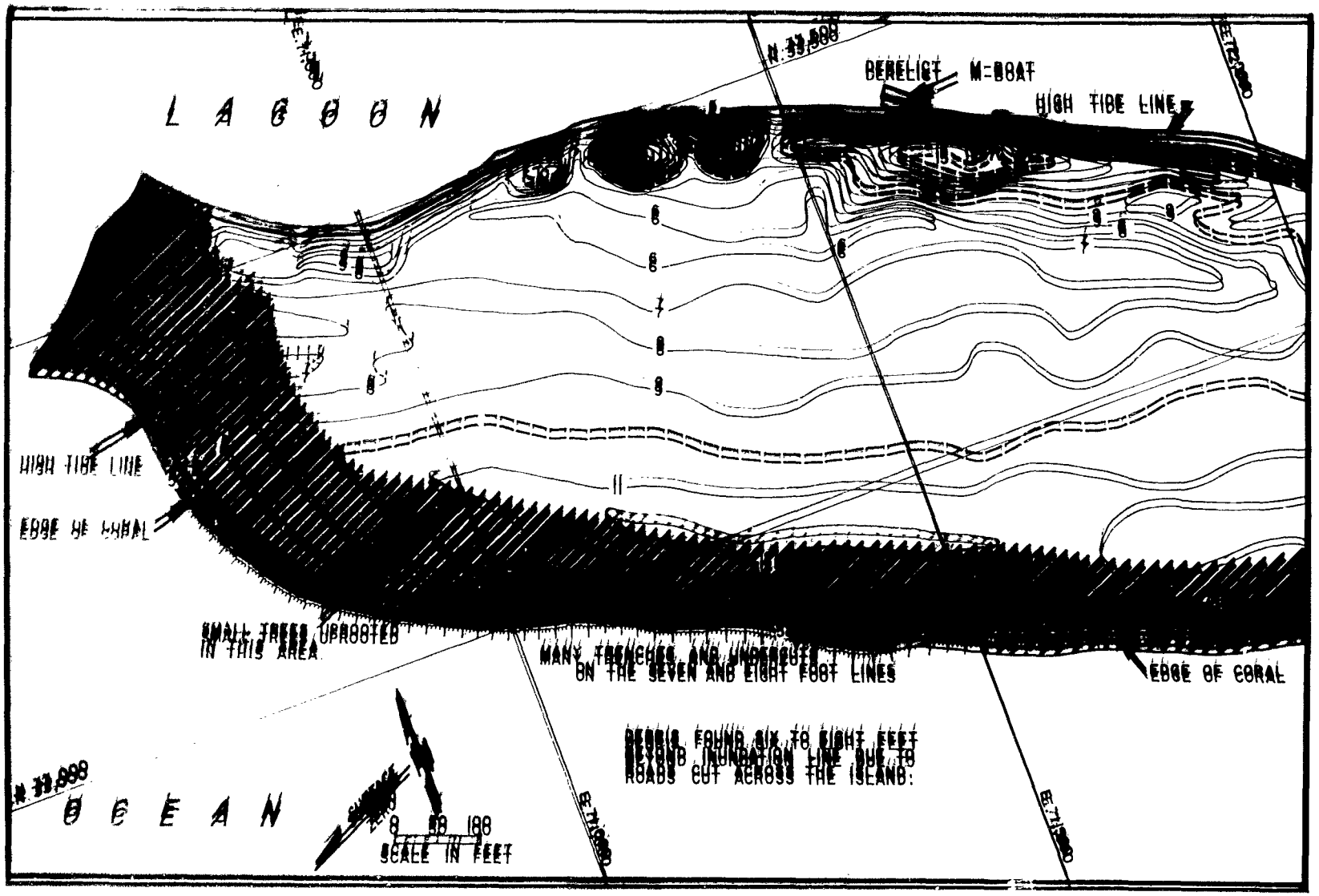

Figure A:6 Wahoo inundation chart: Henry. Entire island beach sandy except where noted as coral.

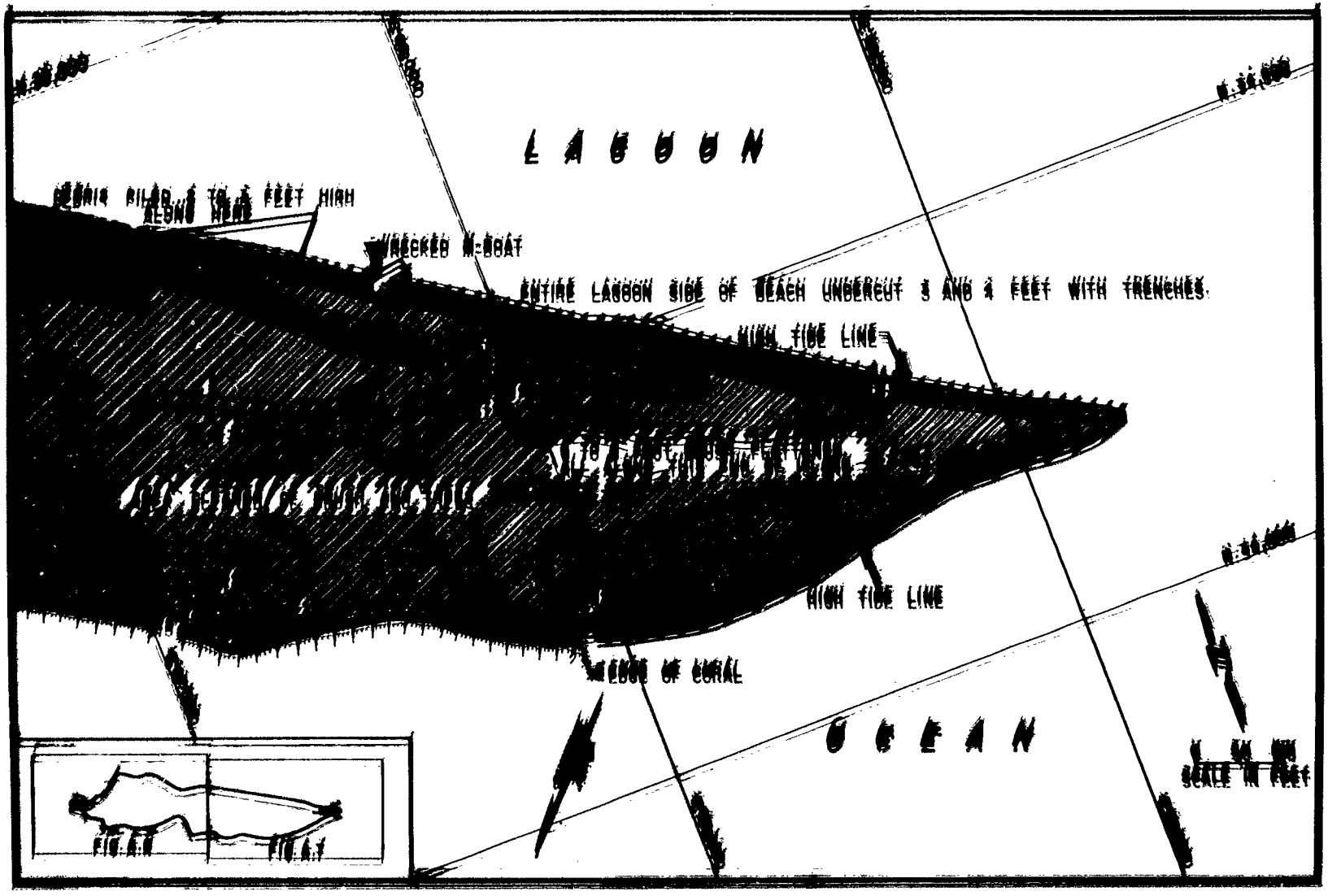

Figure A.7 Wahoo inundation chart: Irwin. Scattered brush along lagoon face with dense brush on both ends.

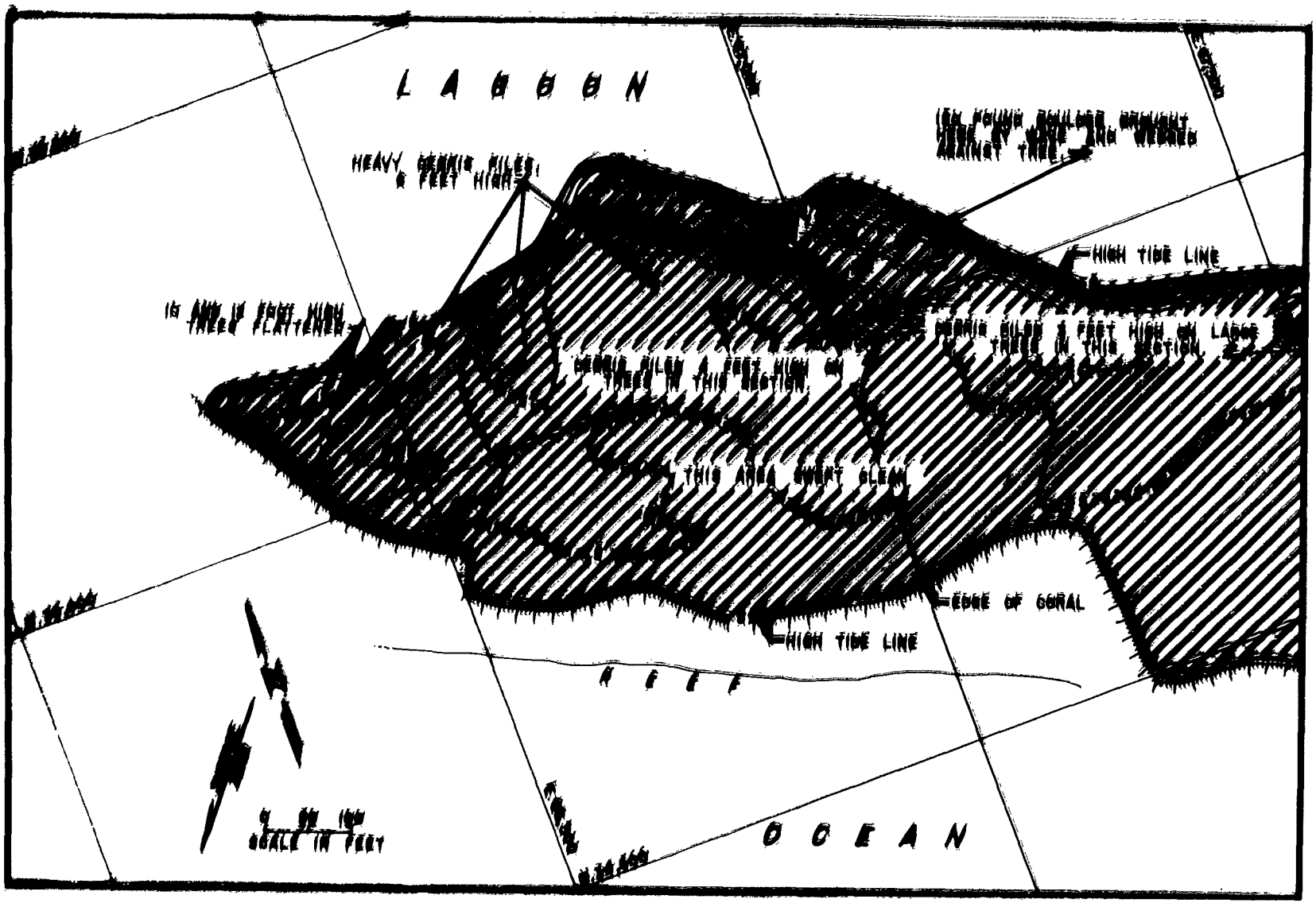

Figure A.8 Wahoo inundation chart: Irwin. Scattered brush along lagoon face with dense brush on both ends.

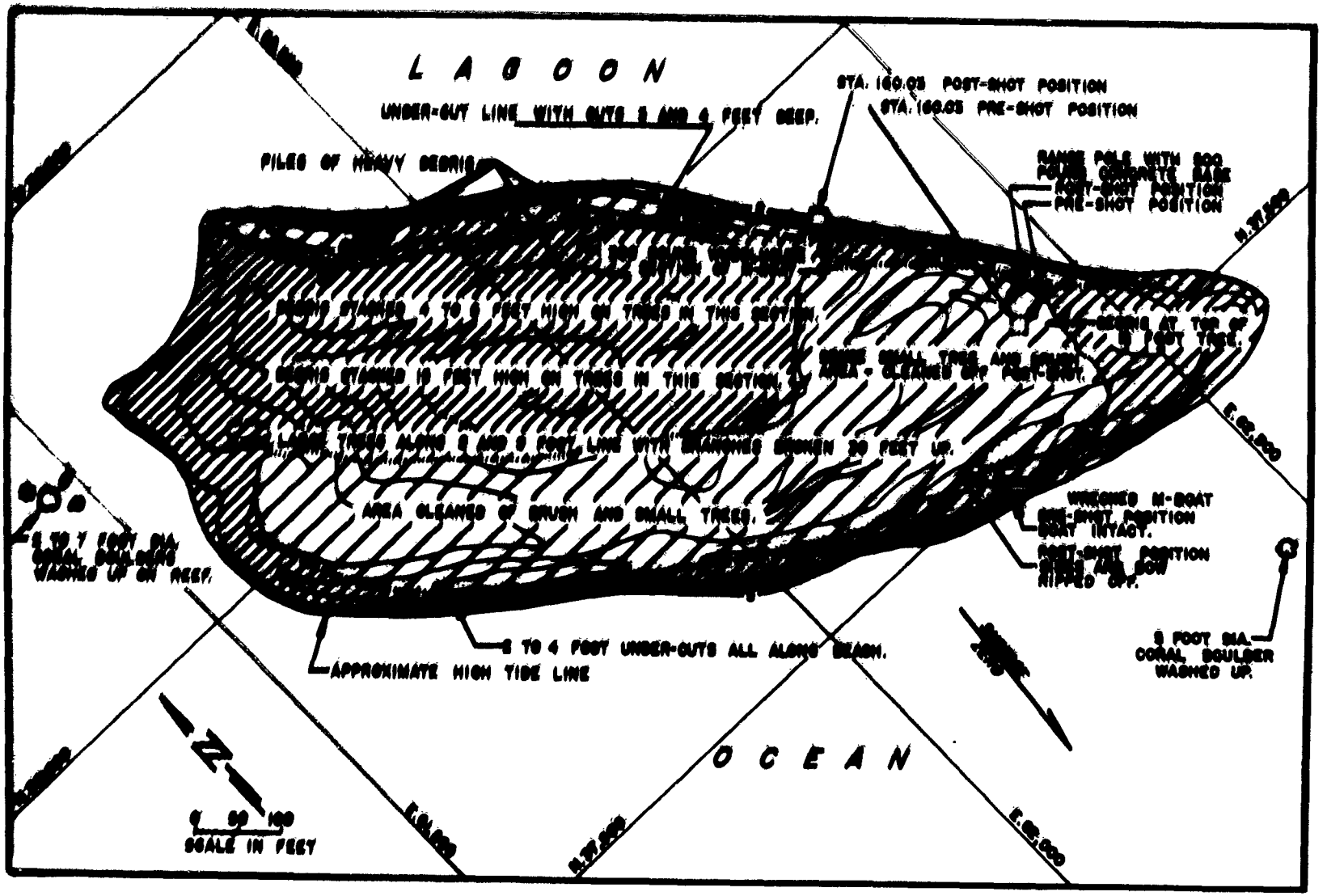

Figure A.9 Wahoo inundation chart: James. Northwest portion of James densely vegetated; remainder sparsely vegetated.

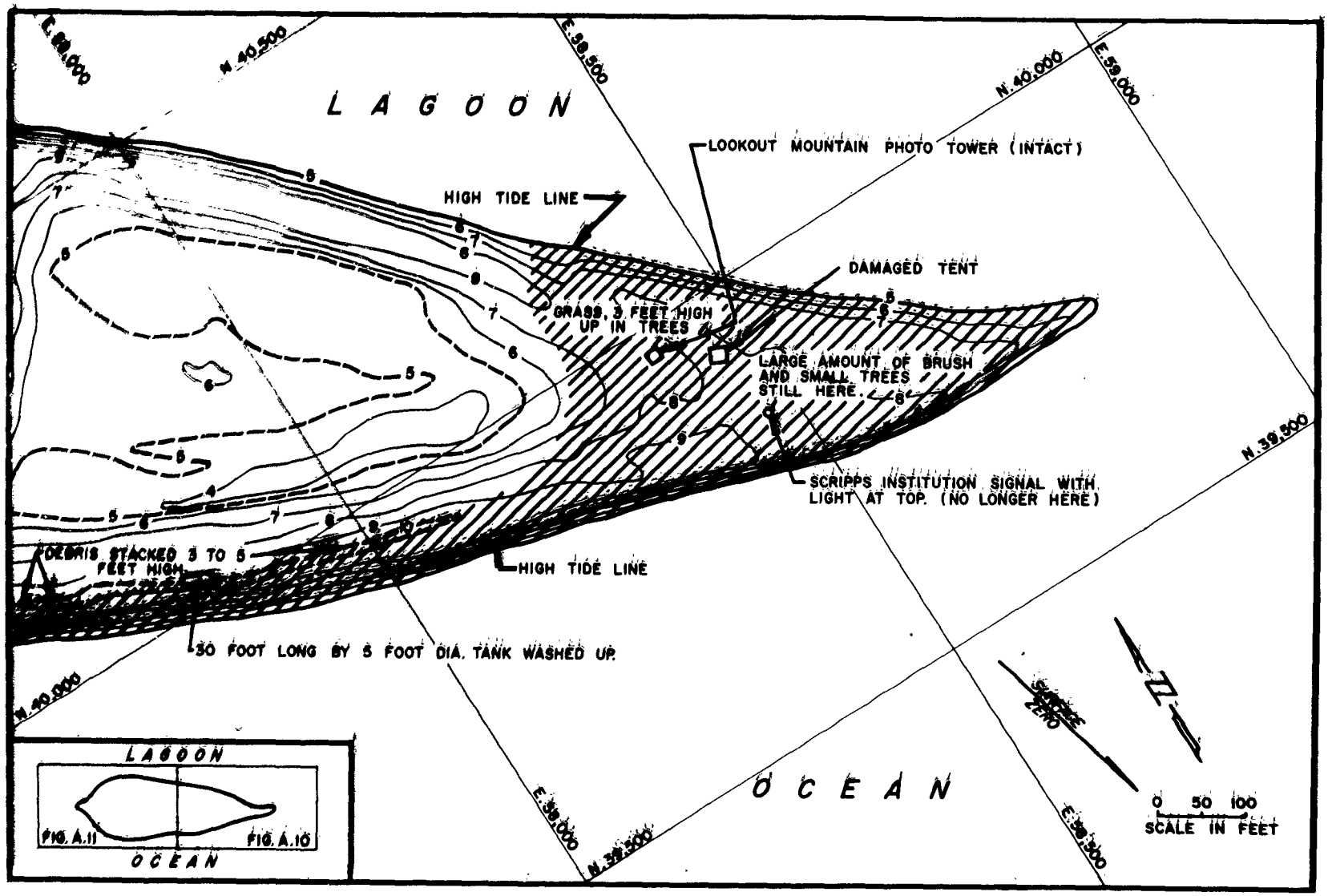

Figure A.10 Wahoo inundation chart: Keith. Entire island surrounded by sandy beach. Coral shelf approximately 15 feet outside high tide line. Northwest two-thirds of island densely vegetated; remainder sparsely vegetated.

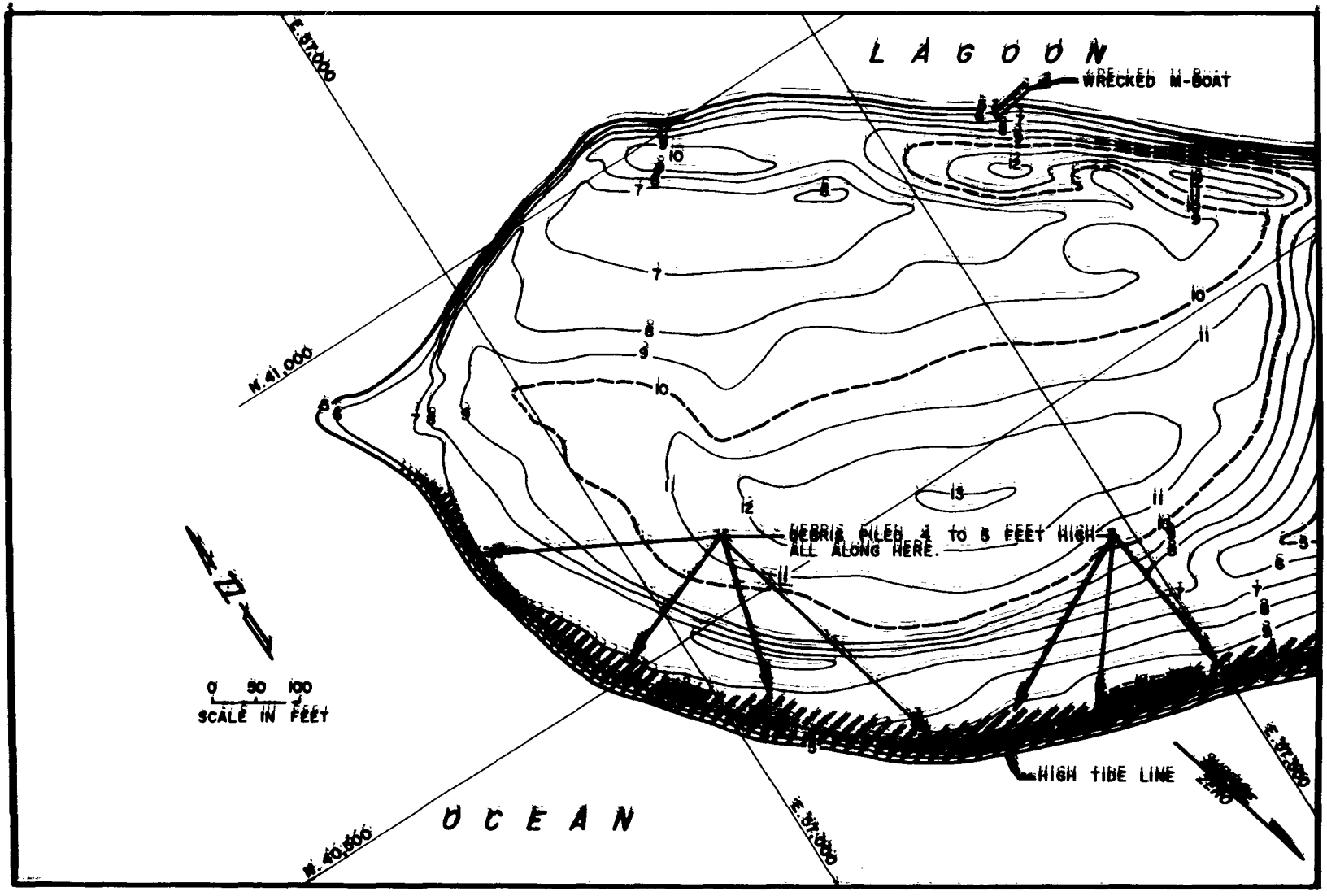

Figure A.11 Wahoo inundation chart: Keith. Entire island surrounded by sandy beach. Coral shelf approximately 15 feet outside high tide line. Northwest two-thirds of island densely vegetated; remainder sparsely vegetated.

Figure A.12 Pre-Wallop East Henry, viewed from ocean.

Figure A.13 Post-Wahoo! East Henry, viewed from ocean.

Figure A.14 Pre-Wahoo west trwin, viewed from ocean.

Figure A.15 Post-Wahoo: west Irwin, viewed from ocean.

Figure A.10 Pre Walloon central level, viewed from south.

Figure A.17 Post Wallow: [illegible] [illegible], viewed from [illegible].

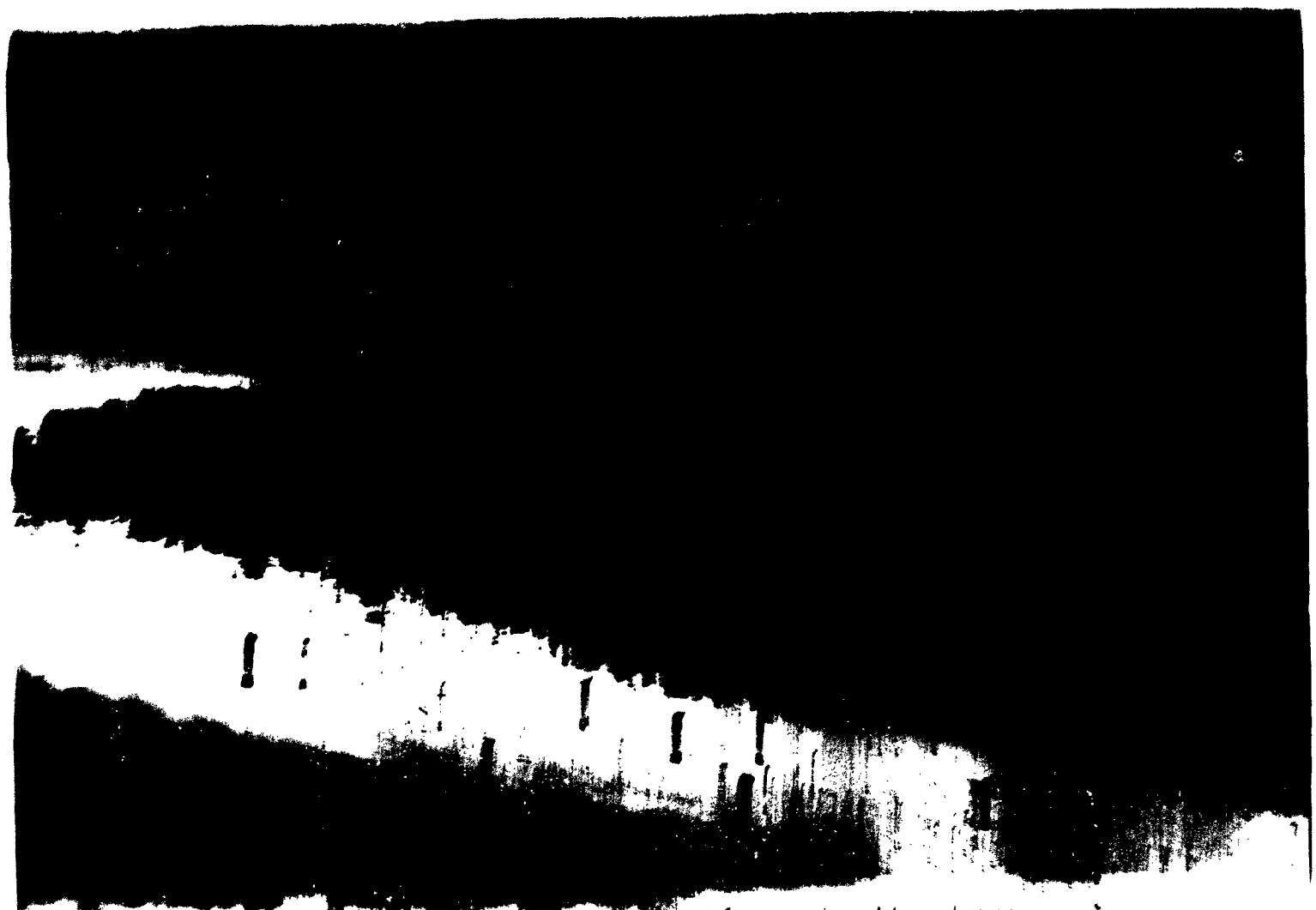

Figure 4-15. Pre-Wallum southeast James, viewed from lagoon.

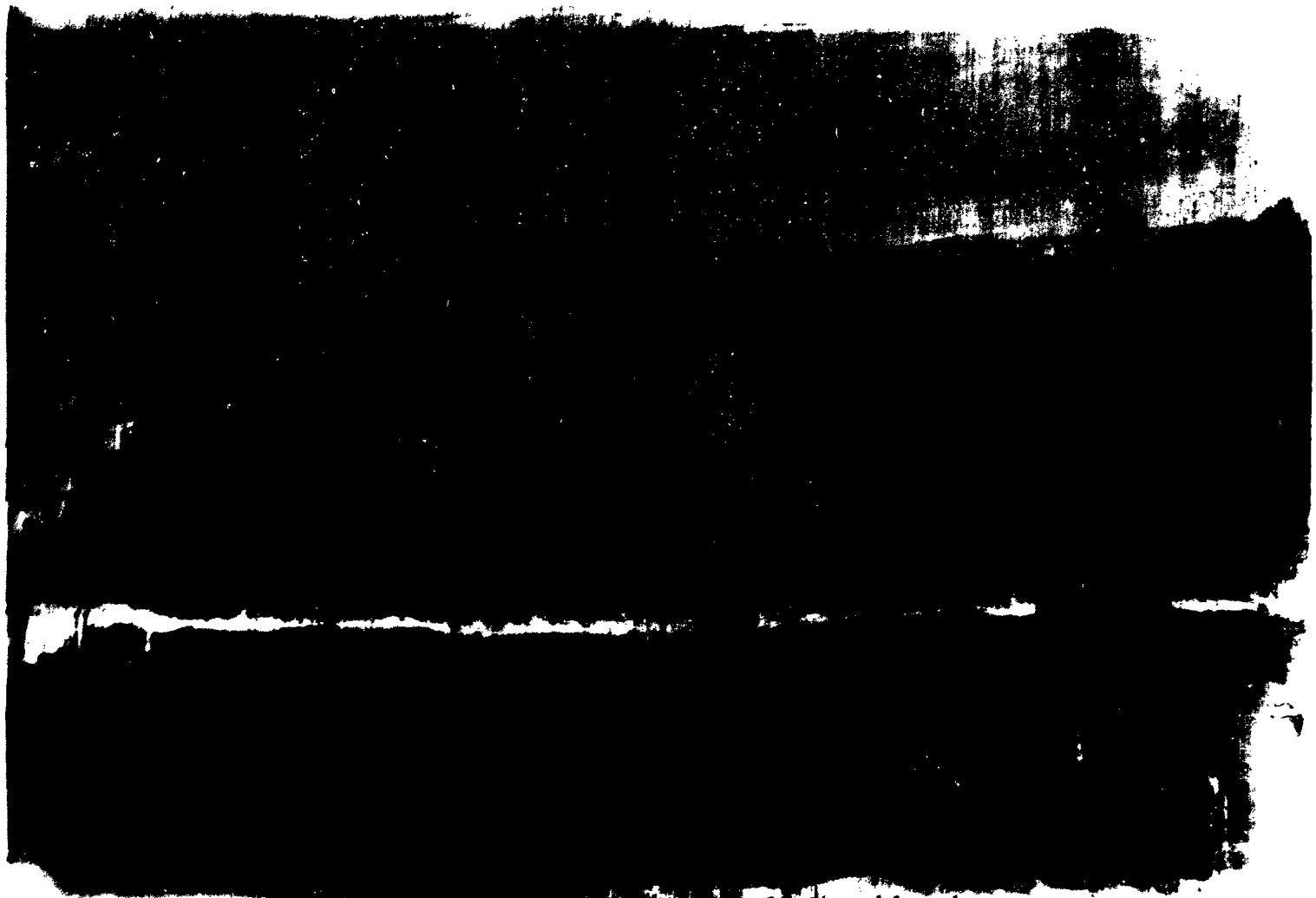

[illegible] viewed from lagoon.
[illegible] wave height poles on beach at left and in water at right.

Figure A.10 Koa-Wahoo: southeast dames, viewed from lagoon.
Note Project 1.6 instrument and camera station in water.

Figure A.21 Pre-Wahoo: southeast James, viewed from ocean.

Figure A.22 Post-Wahoo: southeast James, viewed from ocean. Postshot locations of wave-height poles and instrument and camera station can be seen on far side of island.

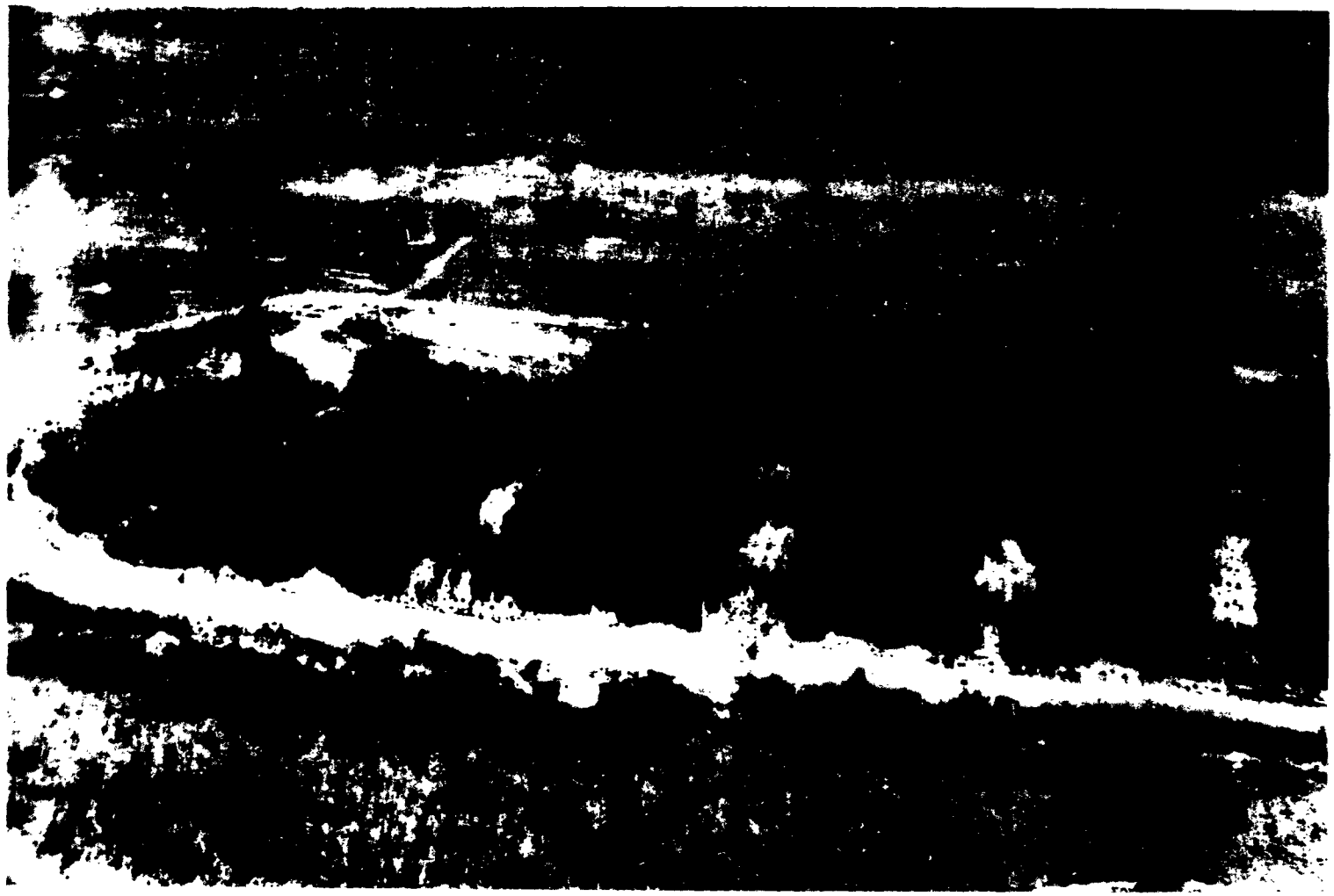

Figure A.23 Pre-Wahoo: northwest James, viewed from ocean.

Figure A.24 Post-Wahoo: northwest James, viewed from ocean.

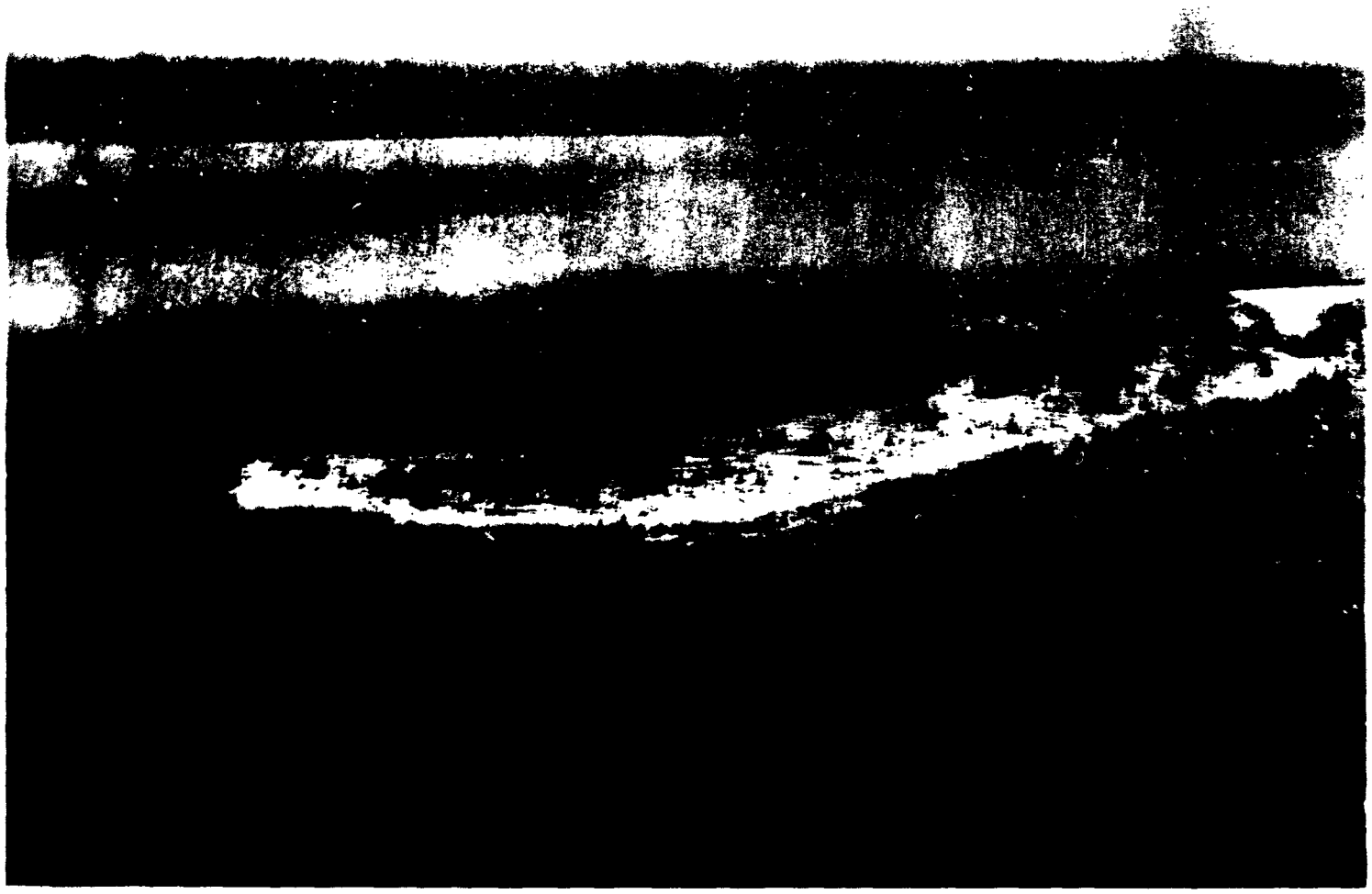

Figure A.25 Post-Wahoo: James, looking east.

Figure A.26 Pre-Wahoo: southeast Keith, viewed from ocean.

Figure A.27 Post-Wahoo: southeast Keith, viewed from ocean.

Figure A.28 Wahoo! First crest arrival at James-Irwin reef.

Figure A.29 Wahoo: Second crest arrival at James-Irwin reef.

Figure A.30 Wahoo: Third crest arrival at James-Irwin reef.

Appendix B

A DISCREPANCY IN ENERGIES AS PREDICTED BY REFERENCE 1

It has been noticed that in the theory of Reference 1 the energy contained in the predicted wave train is approximately twice the energy of the initial water crater postulated as the source of the wave train.

The potential energy W of a cylindrically symmetric elevation E(r) in the surface of an ocean of infinite extent is

$$W = \pi \rho g \int_0^\infty E(r)^2 \, r dr \tag{B.1}$$

The energy of a deep water wave train whose crests and troughs are each sinusoidal is given by

$$Q = \rho g^2 \tau \Sigma (H_n B_n)^2 \tag{B.2}$$

where H_n is the height and B_n the half-period of the n^{th} crest or trough.

Now the waves predicted by Reference 1 are of the form

$$\cos 2\pi (t/T - r/\lambda) \tag{B.3}$$

They may be considered deep water waves when

$$h/\lambda - (\sigma/2\pi) > 1/2 \tag{B.4}$$

Under this condition Equation B.3 becomes

$$\cos (g/4r) t^2 \tag{B.5}$$

The energy of the n^{th} crest or trough of Equation B.5 is

$$Q = 2 r \rho g C \int_{T/2} \cos^2 (g/4r) t^2 \, dt \tag{B.6}$$

Comparison of the results of numerical integration of Equation B.6 with Equation B.2 shows that, for waves whose half-period is less than their age, Equation B.2 is a good approximation (within 5 percent) for Equation B.6. (The age of the wave could be defined as the time from the initial disturbance until the first phase zero of the wave.) Thus, if the waves can be considered to be in deep water, they can be considered sinusoidal for the purpose of energy calculations.

The following is given as a numerical example of the discrepancy. As an initial disturbance, a paraboloid is taken whose radius is R = 785 feet, and whose maximum depth is η = 213 feet. The potential energy of this paraboloid is, from Equation B.1,

$$W = \pi/6 \, \rho g R^2 \eta^2 = 9.4 \times 10^{11} \text{ ft-lb} \tag{B.7}$$

However, by Equation B.2, the energy of the calculated waves in the first group is $Q = 17.4 \times 10^{11}$ ft-lb. The inclusion or an estimate of the energy remaining in the following (much smaller) group results in $W \approx 1/2 \, Q$.

A similar energy discrepancy can be seen in the examples (cylindrical elevation, and paraboloidal impulse) given in Reference 1.

REFERENCES

1. H. C. Kranzer and J. B. Keller; "Water Waves Produced by Explosions"; IMM-NYU 222, September 1955; New York University, Institute of Mathematical Sciences, New York City, New York; Unclassified.

2. T. D. J. Leech; "Project 'Seal': The Generation of Waves by Means of Explosives; Final Report"; December 1950; Department of Scientific and Industrial Research, Wellington, New Zealand; Secret.

3. "Underwater Explosion Research; Vol. II: The Gas Globe"; 1950; Office of Naval Research, Department of the Navy, Washington, D. C.; Unclassified.

4. L. W. Kidd; "Direct Water Wave Measurements"; Project 1.9a, Operation Redwing, WT-1969, 1961; University of California, Scripps Institution of Oceanography, La Jolla, California; Secret Formerly Restricted Data.

5. J. E. Prins; "Characteristics of Waves Generated by a Local Disturbance"; Series 99, Issue 1, August 1956; Wave Research Laboratory, Institute of Engineering Research, Department of Engineering, University of California, Berkeley, California; Unclassified.

6. L. W. Kidd; "Measurement of Secondary Effects: Water Waves"; Project 2.9, Operation Wigwam, WT-1020, 31 July 1959; University of California, Scripps Institution of Oceanography, La Jolla, California; Confidential Formerly Restricted Data.

7. R. L. Wiegel; "Gravity Waves: Table of Functions"; February 1954; Council on Wave Research, The Engineering Foundation, Berkeley, California; Unclassified.

DISTRIBUTION

Military Distribution Category 16

ARMY ACTIVITIES

1 Deputy Chief of Staff for Military Operations, D/A, Washington 25, D.C. ATTN: Dir. of [redacted]
2 Chief of Research and Development, D/A, Washington 25, D.C. ATTN: Atomic Div.
3 Assistant Chief of Staff, Intelligence, D/A, Washington 25, D.C.
4 Chief of Engineers, D/A, Washington 25, D.C. ATTN: [redacted]
5 Chief of Engineers, D/A, Washington 25, D.C. ATTN: [redacted]
6 Chief of Engineers, D/A, Washington 25, D.C. ATTN: [redacted]
7– 9 Commanding General, U.S. Continental Army Command, Ft. Monroe, Va.
10 Director of Special Weapons Development Office, Headquarters CONARC, Ft. Bliss, Tex. ATTN: Capt. Chester I. Peterson
11 President, U.S. Army Artillery Board, Ft. Sill, Okla.
12 President, U.S. Army Air Defense Board, Ft. Bliss, Tex.
13 Commandant, U.S. Army Command & General Staff College, Ft. Leavenworth, Kansas. ATTN: [redacted]
14 Commanding General, Chemical Corps Training Comd., Ft. McClellan, Ala.
15 Commanding General, The Engineer Center, Ft. Belvoir, Va. ATTN: Asst. Cmdt, Engr. School
16 Director, Armed Forces Institute of Pathology, Walter Reed Army Med. Center, 625 16th St., NW, Washington 25, D.C.
17 Commanding Officer, U. S. Army Research Lab., Ft. Knox, Ky.
18 Commandant, Walter Reed Army Inst. of Res., Walter Reed Army Medical Center, Washington 25, D.C.
19– 20 Commanding Officer, Chemical Warfare Lab., Army Chemical Center, Md. ATTN: Tech. Library
21 Commanding General, Engineer Research and Dev. Lab., Ft. Belvoir, Va. ATTN: Chief, Tech. Support Branch
22 Director, Waterways Experiment Station, P.O. Box 631, Vicksburg, Miss. ATTN: Library
23 Commanding General, Aberdeen Proving Grounds, Md. ATTN: Director, Ballistics Research Laboratory
24 Director, Operations Research Office, Johns Hopkins University, 6935 Arlington Rd., Bethesda 14, Md.
25 President, Beach Erosion Board, Corps of Engineers, U.S. Army, 5201 Little Falls Rd., N.W., Washington 16, D.C.
26 Commander-in-Chief, U.S. Army Pacific, APO 958, San Francisco, Calif. ATTN: Ordnance Officer

NAVY ACTIVITIES

27– 28 Chief of Naval Operations, D/N, Washington 25, D.C. ATTN: OP-03EG
29 Chief of Naval Operations, D/N, Washington 25, D.C. ATTN: OP-31
30 Chief of Naval Operations, D/N, Washington 25, D.C. ATTN: OP-75
31 Chief of Naval Operations, D/N, Washington 25, D.C. ATTN: OP-91
32 Chief of Naval Operations, D/N, Washington 25, D.C. ATTN: OP-[illegible]
33– [illegible] Chief of Naval Research, D/N, Washington 25, D.C. ATTN: Code [illegible]
[illegible]– 37 Chief, Bureau of Naval Weapons, D/N, Washington 25, D.C. ATTN: RU[illegible]
38 Chief, Bureau of Ordnance, D/N, Washington 25, D.C.
39 Chief, Bureau of Ships, D/N, Washington 25, D.C. ATTN: Code [illegible]
40 Chief, Bureau of Supplies and Accounts, D/N, Washington 25, D.C.
41 Chief, Bureau of Yards and Docks, D/N, Washington 25, D.C. ATTN: D-440
42 Director, U.S. Naval Research Laboratory, Washington 25, D.C. ATTN: Mrs. Katherine H. Coss
43– 44 Commander, U.S. Naval Ordnance Laboratory, White Oak, Silver Spring 19, Md.
45 Commanding Officer and Director, Navy Electronics Laboratory, San Diego 52, Calif.
46 Commanding Officer, U.S. Naval Mine Defense Lab., Panama City, Fla.
47– 48 Commanding Officer, U.S. Naval Radiological Defense Laboratory, San Francisco, Calif. ATTN: Tech. Info. Div.
49– 50 Commanding Officer and Director, U.S. Naval Civil Engineering Laboratory, Port Hueneme, Calif. ATTN: Code L31
51 Commanding Officer, U.S. Naval Schools Command, U.S. Naval Station, Treasure Island, San Francisco, Calif.
52 Superintendent, U.S. Naval Postgraduate School, Monterey, Calif.
53 Commanding Officer, U.S. Fleet Sonar School, U.S. Naval Base, Key West, Fla.
54 Commanding Officer, U.S. Fleet Sonar School, San Diego 47, Calif.
55 Officer-in-Charge, U.S. Naval School, CEC Officers, U.S. Naval Construction Bn. Center, Port Hueneme, Calif.
56 Commanding Officer, Nuclear Weapons Training Center, Atlantic, U.S. Naval Base, Norfolk 11, Va. ATTN: Nuclear Warfare Dept.
57 Commanding Officer, Nuclear Weapons Training Center, Pacific, Naval Station, San Diego, Calif.
58 Commanding Officer, U.S. Naval Damage Control Tng. Center, Naval Base, Philadelphia 12, Pa. ATTN: ABC Defense Course
59 Commanding Officer, Naval Air Material Center, Philadelphia 12, Pa. ATTN: Technical Data Br.
60 Commanding Officer, U.S. Naval Medical Research Institute, National Naval Medical Center, Bethesda, Md.
61– 62 Commanding Officer and Director, David W. Taylor Model Basin, Washington 7, D.C. ATTN: Library
63 Commanding Officer and Director, U.S. Naval Engineering Experiment Station, Annapolis, Md.
64 Commander, Norfolk Naval Shipyard, Portsmouth, Va. ATTN: Underwater Explosions Research Division
65 Commandant, U.S. Marine Corps, Washington 25, D.C. ATTN: Code AO5H
66 Director, Marine Corps Landing Force, Development Center, MCS, Quantico, Va.
67 Commanding Officer, U.S. Naval CIC School, U.S. Naval Air Station, Glynco, Brunswick, Ga.
68 Chief of Naval Operations, Department of the Navy, Washington 25, D.C. ATTN: OP-04[illegible]
69– 71 Chief, Bureau of Naval Weapons, Navy Department, Washington 25, D.C. ATTN: RR[illegible]

AIR FORCE ACTIVITIES

72 Air Force Technical Application Center, Hq. USAF, Washington 25, D. C.
73 Hq. USAF, ATTN: Operations Analysis Office, Office, Vice Chief of Staff, Washington 25, D. C.
74– 84 Hq. USAF, Washington 25, D.C. ATTN: AFTAC-[illegible]
85 Director of Research and Development, DCS/D, Hq. USAF, Washington 25, D.C. ATTN: Guidance and Weapons Div.
86 The Surgeon General, Hq. USAF, Washington 25, D.C. ATTN: Bio.-Def. Res. Med. Division
87 Commander, Tactical Air Command, Langley AFB, Va. ATTN: Doc. Security Branch
88 Commander, Hq. Air Research and Development Command, Andrews AFB, Washington 25, D.C. ATTN: [illegible]

SECRET

89 Commander, Air Force Ballistic Missile Div. HQ. ARDC, Air Force Unit Post Office, Los Angeles 45, Calif. ATTN: WDSOT
90- 91 Commander, AF Cambridge Research Center, L. G. Hanscom Field, Bedford, Mass. ATTN: CRQST-2
92- 96 Commander, Air Force Special Weapons Center, Kirtland AFB, Albuquerque, N. Mex. ATTN: Tech. Info. & Intel. Div.
97- 98 Director, Air University Library, Maxwell AFB, Ala.
99 Commander, Lowry Technical Training Center (TW), Lowry AFB, Denver, Colorado.
100-102 Commander, Wright Air Development Center, Wright-Patterson AFB, Dayton, Ohio. ATTN: WCACT (For WCOSI)
103-104 Director, USAF Project RAND, VIA: USAF Liaison Office, The RAND Corp., 1700 Main St., Santa Monica, Calif.
105 Commander, Air Technical Intelligence Center, USAF, Wright-Patterson AFB, Ohio. ATTN: AFCIN-4Bla, Library
106 Assistant Chief of Staff, Intelligence, HQ. USAFE, APO 633, New York, N.Y. ATTN: Directorate of Air Targets
107 Commander-in-Chief, Pacific Air Forces, APO 953, San Francisco, Calif. ATTN: PFCIE-MB, Base Recovery

OTHER DEPARTMENT OF DEFENSE ACTIVITIES

108 Director of Defense Research and Engineering, Washington 25, D.C. ATTN: Tech. Library
109 Chairman, Armed Services Explosives Safety Board, DOD, Building T-7, Gravelly Point, Washington 25, D.C.
110 Director, Weapons Systems Evaluation Group, Room 1E880, The Pentagon, Washington 25, D.C.
111-114 Chief, Defense Atomic Support Agency, Washington 25, D.C. ATTN: Document Library
115 Commander, Field Command, DASA, Sandia Base, Albuquerque, N. Mex.
116 Commander, Field Command, DASA, Sandia Base, Albuquerque, N. Mex. ATTN: FCTG
117-118 Commander, Field Command, DASA, Sandia Base, Albuquerque, N. Mex. ATTN: FCWT
119 Commander-in-Chief, Strategic Air Command, Offutt AFB, Neb. ATTN: OAMB
120 U.S. Documents Officer, Office of the United States National Military Representative - SHAPE, APO 55, New York, N.Y.

ATOMIC ENERGY COMMISSION ACTIVITIES

121-123 U.S. Atomic Energy Commission, Technical Library, Washington 25, D.C. ATTN: For DMA
124-125 Los Alamos Scientific Laboratory, Report Library, P.O. Box 1663, Los Alamos, N. Mex. ATTN: Helen Redman
126-130 Sandia Corporation, Classified Document Division, Sandia Base, Albuquerque, N. Mex. ATTN: H. J. Smyth, Jr.
131-140 University of California Lawrence Radiation Laboratory, P.O. Box 808, Livermore, Calif. ATTN: Clovis G. Craig
141 Office of Technical Information Extension, Oak Ridge, Tenn. (Master)
142-175 Office of Technical Information Extension, Oak Ridge, Tenn. (Surplus)